1968

On a New Approach to Rarefied Flow With Applications to Certain Classicalproblems.

Edwin Price Russo
Louisiana State University and Agricultural & Mechanical College

ON A NEW APPROACH TO RAREFIED FLOW

WITH APPLICATIONS TO CERTAIN CLASSICAL PROBLEMS

A Dissertation

Submitted to the Graduate Faculty of the
Louisiana State University and
Agricultural and Mechanical College
in partial fulfillment of the
requirements for the degree of
Doctor of Philosophy

in

The Department of Mechanical, Aerospace
and Industrial Engineering

by
Edwin Price Russo
B.S., Tulane University, New Orleans, Louisiana, 1960
M.S., Tulane University, New Orleans, Louisiana, 1962
January, 1968

ACKNOWLEDGEMENT

This research was conducted under the guidance of Dr. Ozer A. Arnas, Associate Professor of Mechanical Engineering. I want to express my appreciation to him for the consideration and encouragement shown throughout this study.

I also wish to thank Mrs. Annette Mertens for typing the manuscript.

Special acknowledgement is given to my wife, Patricia. Her sacrifices, patience and help were very important contributions in everything that was done.

TABLE OF CONTENTS

LIST OF TABLES

LIST OF FIGURES

NOMENCLATURE

A Cross sectional area, also used as a constant.

a Speed of sound, also used as the length of a side of a rectangular duct.

b Length of the side of a rectangular duct, or of a triangular duct.

c Constant, defined by Equation II-14, $c = \mu_w \rho_w / \mu_\infty \rho_\infty$.

C_D Coefficient of drag, defined by Equation II-31.

c_F Skin friction, defined by Equations II-29 and IV-57.

cos Cosine function.

cosh Hyperbolic cosine function.

erf Error function.

erfc Co-error function.

exp Exponentional function.

f Universal function used in Chapter IV.

G Scale factor, defined by Equations IV-34 and IV-37.

h Perpendicular distance between plates in continuum Couette flow.

h_1 Perpendicular distance between plates in rarefied Couette flow.

i Imaginary numbers equal to $(-1)^{\frac{1}{2}}$.

K Knudsen number, $K = \lambda/L$

k Dimensionless constant = 2.888.

L Characteristic dimension, also used as length of plate.

M Mach number, $M = U/a$.

m Summation index, also used in wedge analysis as equivalent to $\beta/(2-\beta)$.

n Summation index in Equation III-4; ratio of the sides of rectangular duct in Equation III-31.

p Pressure.

R Radius of tube in continuum flow.

R_1 Radius of tube in rarefied flow.

r Radius, also radial coordinate.

Re Reynolds number, $Re = LU/\nu$.

sin Sine function.

sinh Hyperbolic sine function.

t Time.

U Free stream velocity.

u Velocity component.

V Velocity vector, $V = u\vec{i} + v\vec{j} + w\vec{k}$.

v Velocity component.

W Complex potential.

w Velocity component.

x Space coordinate measured along surface in direction of flow.

y Space coordinate measured normal to surface.

z Space coordinate measured along surface in a direction transverse to the flow.

α Angle, also a constant used in Equation IV-35 and defined by Equation IV-36.

β Angle at which separation occurs, Equation IV-25, also a constant used in Equation IV-35 and defined by Equation IV-36, also used as wedge angle, divided by π.

γ Ratio of specific heats, also used as an angle.

ζ Parameter defined by Equation II-23.

η Parameter defined by Equations II-18, IV-6, IV-12 and IV-34.

$\varkappa$ Separation distance between continuum and non-continuum surfaces.

Λ Pressure drop coefficient, defined by Equation III-36.

λ Mean free path, Equation I-1 and I-3.

μ Dynamic viscosity coefficient.

ν Kinematic viscosity.

ξ Nondimensional variable equal to x/L.

π Pi, equal 3.1415926536.

ρ Density.

σ Reflection coefficient.

τ Shear stress.

φ Angle, also pressure drop correction coefficient

ψ Function defined by Equation II-8, or Equation IV-32.

Subscript

D Drag.

F Denotes friction i.e. c_F = skin friction.

k Dummy index = 1,2,3,... .

m Mean velocity in Equation I-1, and summation index.

r Denotes radial component.

s Denotes slip condition, i.e. u_s = slip velocity.

Subscript (cont'd)

w Parameter evaluated at the wall.

z Denotes axial component.

η Parameter evaluated at separation distance.

ϕ Denotes angular component.

∞ Parameter evaluated at free stream conditions.

Superscript

$*$ Parameter evaluated at free stream conditions, or parameter evaluated at separation distance (e.g.η^*).

ABSTRACT

The application of a new mathematical technique to the solution of rarefied flow problems in the slip flow regime is presented. The analysis is based on a new approach to applying the boundary conditions. Instead of applying the slip velocity boundary condition in the conventional manner, a slipping surface is superimposed on a fictitious, continuum, nonslipping surface. These surfaces are separated by a distance which is proportional to the degree of slip. This approach is very desirable since it provides solutions without encountering the mathematical difficulties of solving a partial differential equation with nonhomogeneous boundary conditions.

The flow problems considered are:

1) Rayleigh flow - flow over a flat plate
2) Couette flow - flow between two parallel flat plates which are moving relative to each other
3) Poiseuille flow - flow through a pipe
4) Flow through a rectangular cross section duct
5) Flow through a triangular cross section duct
6) Flow past a right circular cylinder using Blasius' approach

7) Flow past a wedge

The solutions given for cases 1,2,3 and 6 above are compared to experimental data taken from the literature. In cases 4, 5 and 7 the author could find no applicable experimental data.

During the analysis of the rarefied flow past a cylinder, a new continuum result for the skin-friction drag coefficient was obtained. A value of $6(Re)^{-\frac{1}{2}}$ was obtained using Blasius' exact approach to the problem; whereas, a value of $4(Re)^{-\frac{1}{2}}$, which is obtained by approximate means, is usually cited in the literature. The analysis leading to the result of $6(Re)^{-\frac{1}{2}}$ is given in Appendix C.

CHAPTER I

INTRODUCTION

The subject of this dissertation deals with the solutions of some rarefied flow problems, and utilizes the Navier-Stokes equations as a basis. Rarefied flow problems differ from ordinary continuum problems in that the velocity of the gas adjacent to the surface considered is not zero but is slipping along the surface. The difference in the analyses to be carried out here and in other analyses of rarefied flows lies in the technique of the application of this slip velocity boundary condition to these problems.

The mechanics of rarefied gases has been the subject of many investigations since the time of Maxwell (1). Until comparatively recently, these studies were confined to the case of very slow speeds and in general to internal flow geometries associated with vacuum installations. Since about 1946, there has been considerable revival of interest and activity in the field, largely due to the possibility of flight at very high altitudes and at very high speeds. This activity was given impetus in pioneering articles by Tsien (2,3), which formulated many of the significant problems as well as the general lines of research which have subsequently proved successful.

A rarefied gas flow is a flow in which the length of the molecular mean free path, λ, is comparable to some significant dimension, L, of the flow field. A mean free path is the distance that a molecule will travel before it loses its identity by collision with other molecules. The gas then does not behave entirely as a continuous fluid but rather exhibits some characteristics of its coarse molecular structure. The dimensionless parameter which is considered of paramount importance in the flow of rarefied gases is the Knudsen number, K, which is defined as the ratio of the mean free path, λ, to a characteristic dimension, L. The Knudsen number can also be expressed in terms of more familiar parameters of fluid mechanics, (i.e., the Mach number, $M = U/a$, and the Reynolds number, $Re = LU/\nu$, where U is the free stream velocity, a is the speed of sound and ν is the kinematic viscosity). From kinetic theory (4) one defines the mean free path by the relation

$$\lambda = \frac{2\nu}{v_m} \qquad \text{(I-1)}$$

The mean molecular speed, v_m, is related to the speed, a, as follows:

$$v_m = \left(\frac{8}{\pi\gamma}\right)^{\frac{1}{2}} a \qquad \text{(I-2)}$$

Hence one obtains upon substitution of Equation I-2 into I-1,

$$\lambda = \frac{1.26(\gamma)^{\frac{1}{2}}\nu}{a} \qquad \text{(I-3)}$$

Using this result the Knudsen number, $K = \lambda/L$, can now be expressed as

$$K = \frac{1.26(\gamma)^{\frac{1}{2}}M}{Re} \qquad \text{(I-4)}$$

The flow conditions near the wall for the case in which the Knudsen number is small but not negligible were first investigated by Maxwell in 1879. It was found that the gas immediately adjacent to a solid surface was no longer at rest but had a finite tangential velocity. This type of flow was called a slip flow. If the Knudsen number is very large, one enters an entirely new realm of fluid mechanics. Under this circumstance no boundary layer is formed. Here the chances for the collision of molecules among themselves are much smaller than the chances for the collision of molecules with the surface of the body. One may consequently neglect any distortion of the free stream velocity distribution due to the presence of the body. This realm of fluid mechanics is called free molecule flow. The regime between free molecule flow and slip flow, (i.e., characterized by an intermediate Knudsen number) is called transition flow. The division of fluid mechanics in the aforementioned regimes is not a clear cut problem. Schaaf and Chambre (5) suggest the following

breakdown

$$
\begin{aligned}
.0 &< M/Re < .01 && \text{Continuum} \\
.01 &< M/Re < .1 && \text{Slip Flow} \\
.1 &< M/Re < 3.0 && \text{Transition Flow} \\
3.0 &< M/Re < \infty && \text{Free Molecule Flow}
\end{aligned}
\qquad \text{(I-5)}
$$

This dissertation deals with the slip flow regime; however, the theory presented here also agrees with experimental data taken in the transition regime.

The choice of equations which are applicable for describing rarefied flow phenonema is still an unresolved problem. Kinetic theory is valid for the problems of free molecule rarefied flow. At the other extreme of continuum flow, the Navier-Stokes equations are also integrals of motion of the Boltzmann equation of kinetic theory. Thus it follows that some form of the Boltzmann equation is valid throughout the flow regime from a highly rarefied gas to the conventional gaseous continuum of phenomenological theory. To date, there is no known solution that is generally applicable from the continuum to the free molecule regimes.

There is a considerable and rapidly growing body of experimental data dealing with the problem of slip flow. Excellent summaries of these data can be found in references 5,6,7, and 8. Until recently, it had been generally considered that some kinetic theory modification of the Navier-

Stokes equations, such as the Burnett equations (9) or Grad's Thirteen Moment equations (10), together with slip velocity boundary conditions could be regarded as applicable to the slip flow regime. This view has been held in spite of several well recognized difficulties associated with the Burnett and Thirteen Moment equations, and also of the lack of any experimental verification. Recent experimental and theoretical findings (5,11) now make the validity of these equations appear less likely and in fact seem to indicate that the Navier-Stokes equations, together with slip velocity boundary conditions are not only adequate but probably superior.

Some of the basic difficulties associated with the aforementioned kinetic theory equations are as follows:

1. They are confined to monatomic gases. Since air is composed of diatomic nitrogen and oxygen, this is a serious restriction for aerodynamic applications. Wang-Chang and Uhlenbeck (12) have attempted to develop a kinetic theory approach for polyatomic gases; however, their approach is limited to low temperatures.
2. Experimental evidence (5) seems contrary to either the Burnett or the Thirteen Moment equations.
3. Recent theoretical results (13) also seem contrary to these equations.

4. The order of the Burnett equations is higher than the order of the Navier-Stokes equation; thus an additional boundary condition is required for mathematical compatability. Also, it has not been definitely agreed upon as to which boundary condition this should be.

This dissertation, therefore, utilizes the Navier-Stokes equations as a basis. However, instead of following the traditional approach of using a slip velocity boundary condition, the slipping surface will be superimposed on a fictitious, continuum, nonslipping surface at a distance, η, which is proportional to the degree of slip, Figure I-1. It is felt that this approach is superior to the traditional approach for the following reasons:

1. Any problem which has a continuum solution can be simply extended by this technique to include slip effects; whereas, the traditional method calls for resolving the defining equations with a new non-zero boundary condition (i.e., finite velocity at the wall) which usually causes mathematical difficulties.
2. The experimental data were in better agreement with the theory given by this technique than with traditional theories as shown in the analyses in later chapters.

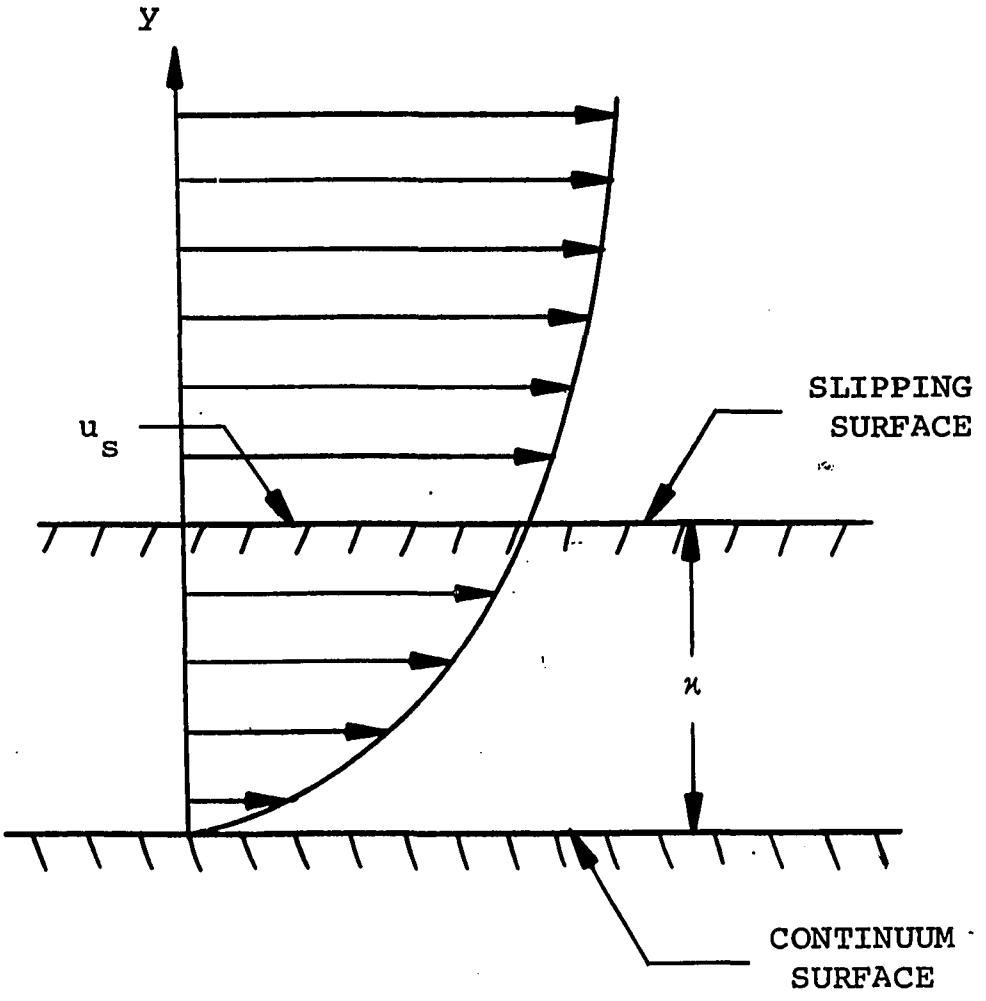

FIGURE I-1 SUPERPOSITION OF SLIPPING AND NONSLIPPING FLAT PLATES FOR RAYLEIGH'S PROBLEM

In this dissertation, the classical Rayleigh, Couette and Poiseuille flow problems are analyzed. The solution for flow past a right circular cylinder is also presented. In analyzing the rarefied cylinder problem a new continuum result for the cylinder skin-friction drag coefficient was discovered and its analysis is given here. Analyses of flow past a wedge and flow through rectangular and triangular ducts are also presented but the results are not given in as much detail as the other problems since very little theoretical or experimental work has been conducted for this type of flow.

CHAPTER II

ANALYSIS

The fact that there is a slip velocity at the interface between a solid and a gas at low pressures has been recognized since the time of Maxwell (1) and Knudsen (14). The following analysis of a monatomic gas adjacent to an isothermal surface serves to relate the slip velocity and the gradient of the tangential velocity. Near the wall the gas consists of molecules, one half of which have just come off the wall, the other half of which have come, on the average, from a layer of gas a mean free path away. If y is the normal coordinate, one has (5)

$$u_w = \frac{1}{2}\left(\left[u_w + \lambda\frac{\partial u}{\partial y}\right)_w\right] + \left\{(1-\sigma)\left[u_w + \lambda\frac{\partial u}{\partial y}\right)_w\right]\right\}\Bigg) \quad \text{(II-1)}$$

where σ is the fraction of diffusely reflected molecules whose average tangential velocity is zero and $(1-\sigma)$ is the fraction of specularly reflected molecules whose average tangential velocity is the same as the molecules incident from the layer a distance equivalent to the mean free path, λ, above the wall. Specular reflection consists of a reversal of the normal velocity component which produces a normal momentum transfer to the surface and leaves the tangential velocity unchanged.

Diffusely reflected molecules are those leaving the surface in random directions and with random velocities. It is these molecules that contribute the tangential momentum transfer to the surface. The reflection coefficient, σ, is tabulated in reference 15.

Equation II-1 reduces to

$$u_w = \frac{2-\sigma}{\sigma} \lambda \frac{\partial u}{\partial y} \Big)_w \qquad \text{(II-2)}$$

It is apparent that slip occurs only when λ is not negligible. The expression for λ is given by Equation I-3.

As pointed out in Chapter I the kinetic theory equations have not met with favorable success in the slip flow regime; hence, the equations best suited for this regime are the usual continuum equations. These equations are

Continuity

$$\frac{\partial \rho}{\partial t} + \text{div}(\rho \vec{V}) = 0 \qquad \text{(II-3)}$$

where ρ is the density and $\vec{V}$ is the velocity vector $(\vec{V} = u\vec{i} + v\vec{j} + w\vec{k})$.

Navier-Stokes (Momentum)

$$\rho\frac{\partial\vec{V}}{\partial t} - \rho\vec{V} \times \vec{\omega} + .5\rho\nabla(\vec{V}\cdot\vec{\omega}) = -\text{grad}(p + \Omega) + \mu[\text{grad}(\text{div}\ \vec{V}) - \text{curl}\ \vec{\omega}] \qquad \text{(II-4)}$$

where p is pressure, Ω is the body force potential, μ is the coefficient of viscosity and

$$\vec{\omega} = \text{curl}\ \vec{V} \qquad \text{(III-5)}$$

An example of the application of these equations to a problem in slip flow will now be analyzed. The flat plate will be used since this is the simplest geometry. The analysis will be based on the Rayleigh problem which involves the definition of the flow field induced by instantaneous acceleration of an infinite flat plate in a viscous medium. Rayleigh's problem is of interest because it is a relatively simple boundary-layer-type flow and may be considered as a model indicating the essential features of the slip effect. A result for the skin-friction on a semi-infinite flat plate is then obtained by relating time in the unsteady state Rayleigh problem to distance in the steady-state problem; thus eliminating the time variable. The solution obtained can then be matched to the usual stationary flat plate problem solution in the continuum. This solution can then be extended to rarefied flow by imposing the non-zero slip

velocity condition at the wall. An abundant supply of literature on the kinetic theory approach to the Rayleigh problem can be found in the works of Yang and Lees (16,17), Lees (18), Gross and Jackson (19,20) Broadwell (21) and Cercignani and Sernagiotto (22,23). The Navier-Stokes approach can be found in the works of Mirels (24), Schaaf (6,25) and Russo and Arnas (26). Mirels and Schaaf approach the problem by applying a slip velocity boundary condition; whereas, the analysis given here and in reference 26 introduces the aforementioned technique of superimposing a slipping flat plate on a fictitious, continuum nonslipping one at a normal distance, κ, proportional to the degree of slip.

Mirels' Solution

By performing an order of magnitude analysis on the governing equations, as is customarily done in boundary layer problems, one arrives at the following conclusions: All gradients and their derivatives in the tangential, x, and transverse, z, directions are small compared with those in the normal, y, direction and hence may be neglected. By application of the Bernoulli equation one can also see that the pressure gradient along the wall is zero. Further, if all types of body forces are assumed to be zero, the governing equations thus become

Continuity

$$\frac{\partial \rho}{\partial t} + \frac{\partial (\rho v)}{\partial y} = 0 \qquad \text{(II-6)}$$

Navier-Stokes

$$\rho \frac{\partial u}{\partial t} + \rho v \frac{\partial u}{\partial y} = \frac{\partial}{\partial y}\left(\mu \frac{\partial u}{\partial y}\right) \qquad \text{(II-7)}$$

Equation II-6 suggests the existence of a function ψ such that

$$\frac{\rho}{\rho_\infty} = \frac{\partial \psi}{\partial y} \qquad \text{(II-8)}$$

and

$$\frac{\rho v}{\rho_\infty} = -\frac{\partial \psi}{\partial t} \qquad \text{(II-9)}$$

where the subscript, ∞, designates conditions far from the wall. Transformation of the independent variables from (t,y) to (t,ψ) is accomplished, as done in references 27 and 28, by the following relations:

$$\left(\frac{\partial}{\partial y}\right)_t = \frac{\partial \psi}{\partial y}\left(\frac{\partial}{\partial \psi}\right)_t = \frac{\rho}{\rho_\infty}\left(\frac{\partial}{\partial \psi}\right)_t \qquad \text{(II-10)}$$

and

$$\begin{aligned}\left(\frac{\partial}{\partial t}\right)_y &= \frac{\partial t}{\partial t}\left(\frac{\partial}{\partial t}\right)_\psi + \frac{\partial \psi}{\partial t}\left(\frac{\partial}{\partial \psi}\right)_t \\ &= \left(\frac{\partial}{\partial t}\right)_\psi - \frac{\rho v}{\rho_\infty}\left(\frac{\partial}{\partial \psi}\right)_t\end{aligned} \qquad \text{(II-11)}$$

With Equations II-10 and II-11 the Navier-Stokes equation becomes

$$\rho\left[\left(\frac{\partial u}{\partial t}\right)_{\psi} - \frac{\rho v}{\rho_\infty}\left(\frac{\partial u}{\partial \psi}\right)_t\right] + \rho v\left[\frac{\rho}{\rho_\infty}\left(\frac{\partial u}{\partial \psi}\right)_t\right] = \frac{\rho}{\rho_\infty}\frac{\partial}{\partial \psi}\left[\mu\frac{\rho}{\rho_\infty}\frac{\partial u}{\partial \psi}\right] \qquad \text{(II-12)}$$

which reduces to

$$\frac{\partial u}{\partial t} = \frac{1}{\rho_\infty}\frac{\partial}{\partial \psi}\left[\frac{\mu\rho}{\rho_\infty}\frac{\partial u}{\partial \psi}\right] \qquad \text{(II-13)}$$

Equation II-13 may be simplified further by considering $\mu\rho/\mu_\infty\rho_\infty$ to be constant throughout the flow field and equal to $\mu_w\rho_w/\mu_\infty\rho_\infty$ (so as to be correct in the vicinity of the wall which is the region of interest). This same simplifying assumption was made by Mirels (24); namely,

$$\frac{\mu\rho}{\mu_\infty\rho_\infty} = \frac{\mu_w\rho_w}{\mu_\infty\rho_\infty} = c \qquad \text{(II-14)}$$

With Equation II-14 values of compressible boundary-layer skin-friction are obtained in reference 29 which agree with the more accurate numerical integrations of reference 30 to within 5 percent for flight conditions up to Mach 5 and within 2 percent for higher speeds.

Substitution of Equation II-14 into Equation II-13 yields

$$\frac{\partial u}{\partial t} = c\,\nu_\infty\frac{\partial^2 u}{\partial \psi^2} \qquad \text{(II-15)}$$

This equation is the general form for the Rayleigh problem. The boundary conditions for the continuum problem are

$$\begin{aligned} u &= U && t = 0 \quad \text{and} \quad \psi > 0 \\ u &= 0 && t \geq 0 \quad \text{and} \quad \psi = 0 \\ u &\to U && t \geq 0 \quad \text{and} \quad \psi \to \infty \end{aligned} \tag{II-16}$$

The solution to Equation II-15 with Equation II-16 is

$$u = U \operatorname{erf}(\eta) \tag{II-17}$$

where

$$\eta = \frac{\psi}{2(c\,\nu_\infty t)^{\frac{1}{2}}} \tag{II-18}$$

The boundary conditions for the case of slip at the wall are

$$\begin{aligned} u &= U && t = 0 \quad \text{and} \quad \psi > 0 \\ u &= \lambda \frac{\rho_w}{\rho_\infty} \frac{\partial u}{\partial \psi}_w && t \geq 0 \quad \text{and} \quad \psi = 0 \\ u &\to U && t \geq 0 \quad \text{and} \quad \psi \to \infty \end{aligned} \tag{II-19}$$

The second condition in Equation II-19 above comes from the definition of the slip velocity u_w as

$$u_w = \lambda \frac{\partial u}{\partial y}\Big)_w \tag{II-20}$$

Here the reflection coefficient, σ, is assumed to be equal to unity, as was in Mirels' (24) analysis. After transformation, using Equations II-8 and II-9

$$u_w = \lambda \frac{\rho_w}{\rho_\infty} \frac{\partial u}{\partial \psi}\Big)_w \tag{II-21}$$

The solution to Equation II-15 with Equation II-19 is

$$u = U\left\{\operatorname{erf}(\eta) + \operatorname{erfc}(\eta + \zeta)\exp\left[\zeta(2\eta + \zeta)\right]\right\} \tag{II-22}$$

where

$$\zeta = \frac{\rho_\infty (c\, \nu_\infty t)^{\frac{1}{2}}}{\lambda \rho_w} \qquad \text{(II-23)}$$

The shear stress at any point in the flow field is

$$\tau = \mu \frac{\partial u}{\partial y} \qquad \text{(II-24)}$$

or using Equations II-8 and II-9

$$\tau = \mu \frac{\rho}{\rho_\infty} \frac{\partial u}{\partial \psi} \qquad \text{(II-25)}$$

which becomes, using Equation II-22,

$$\tau = \frac{\mu_w \rho}{\lambda \rho_w} \left\{ \operatorname{erfc}(\eta + \zeta) \exp[\zeta (2\eta + \zeta)] \right\} \qquad \text{(II-26)}$$

for the case with slip at the wall. The shear stress evaluated at the wall is

$$\tau_w = \frac{\mu_w U}{\lambda} \left[\operatorname{erfc}(\zeta) \exp(\zeta^2) \right] \qquad \text{(II-27)}$$

In order to make the present results for the flat plate skin friction in slip flow match the known flat plate continuum solution when the slip flow solution tends toward the no-slip case, Mirels (24) introduces the transformation $t = kx/U$, where k is a dimensionless constant. It is then possible, by proper choice of k, to match the parameters so that they are identical to the results obtained for a flat plate without slip. Thus k is chosen so that the shear

stress at the wall, as computed above, will exactly match the flat plate solution given in (29). Thus using the transformation, with k = 2.888,

$$t = \frac{2.888x}{U} \qquad \text{(II-28)}$$

which matches the stationary and non-stationary continuum solutions. Rayleigh (31) and Howarth (28) also used a similar transformation in their work. Since the local skin friction coefficient is given by

$$c_F = \frac{2\,\tau_w}{\rho_w U^2} \qquad \text{(II-29)}$$

and using Equation II-27, Equation II-29 becomes

$$(\gamma)^{\frac{1}{2}}\, M^* c_F^* = 1.596\ \text{erfc}\left[\frac{1.356}{M^*}\left(\frac{Re^*}{\gamma}\right)^{\frac{1}{2}}\right] \cdot \exp\left\{1.838\left[\frac{1}{M^{*2}}\left(\frac{Re^*}{\gamma}\right)\right]\right\} \qquad \text{(II-30)}$$

where * parameters are evaluated at the wall. Equation II-30 is plotted in Figure II-1.

The average drag coefficient is defined by

$$C_D^* = \frac{1}{L}\int_0^L c_F^*\,dx \qquad \text{(II-31)}$$

Equation II-30 substituted into Equation II-31 yields

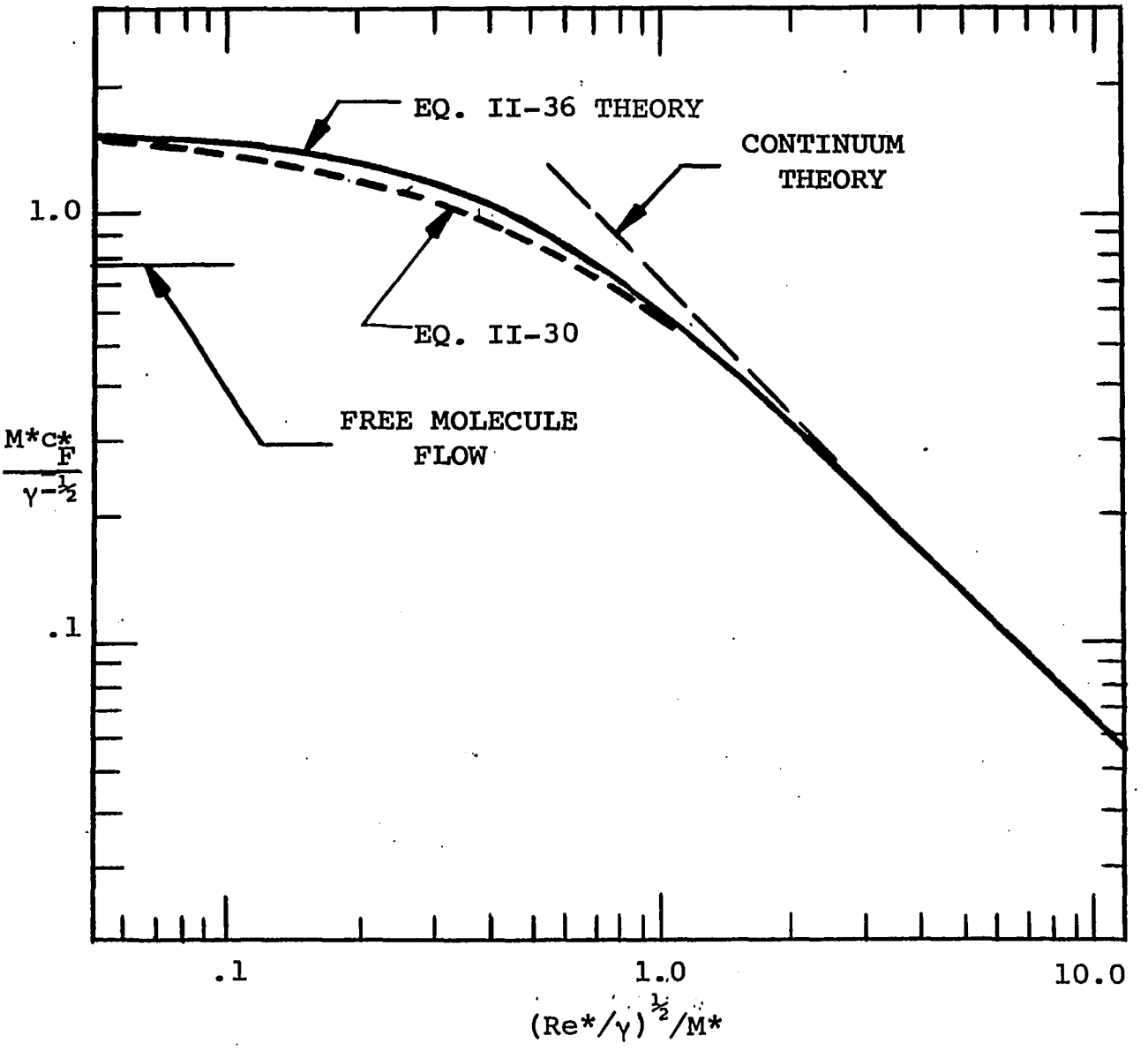

FIGURE II-1 LOCAL SKIN-FRICTION COEFFICIENT ON A FLAT PLATE

$$(\gamma)^{\frac{1}{2}} M^* C_D^* = 0.869 \left[M^* \left(\frac{\gamma}{Re_L^*}\right)\right]^2 \cdot \left\{1.53\left[\left(\frac{Re_L^*}{\gamma}\right)^{\frac{1}{2}} \frac{1}{M^*}\right] - 1 + \operatorname{erfc}\left[1.356 \left(\frac{Re_L^*}{\gamma}\right)^{\frac{1}{2}} \frac{1}{M^*}\right] \cdot \exp\left[1.838 \left\{\left(\frac{Re_L^*}{\gamma}\right)^{\frac{1}{2}} \frac{1}{M^*}\right\}^2\right]\right\} \quad \text{(II-32)}$$

Equation II-32 is plotted in Figure II-2. Equations II-30 and II-32 are the same as those obtained by Mirels (24).

Using the concept of superposition of the slip and non-slip plates, one can arrive at equations similar to Equations II-30 and II-32. In this case, however, the shear stress must be evaluated at $\varkappa$ (see Figure I-1) to give

$$\tau_{\varkappa} = 0.332 \frac{U \mu_{\varkappa}}{x} \left(Re_{\varkappa}\right)^{\frac{1}{2}} e^{-\eta_{\varkappa}^2} \quad \text{(II-33)}$$

where Equations II-17 and II-28 are used. It is to be noted, however, that the state properties evaluated at the wall in Mirels (24) and those evaluated at $\varkappa$ are the same. However, $\eta_{\varkappa}$ equals zero in Mirels' solution. The variable $\eta_{\varkappa}$ may be obtained by noting that the velocity u evaluated at $\eta_{\varkappa}$ must be equal to the slip velocity. After transformation, the value of the slip velocity becomes

$$u = 0.332 \lambda \frac{\rho_w}{\rho_\infty} \left(\frac{U^3}{c \nu_\infty x}\right)^{\frac{1}{2}} e^{-\eta_{\varkappa}^2} \quad \text{(II-34)}$$

Equating this result to Equation II-17 evaluated at $\varkappa$ gives

$$\operatorname{erf}\left(\eta_{\varkappa}\right) e^{\eta_{\varkappa}^2} = 0.416 M^* \left(\frac{\gamma}{Re^*}\right)^{\frac{1}{2}} \quad \text{(II-35)}$$

Numerical values of Equation II-35 are given in Table II-1.

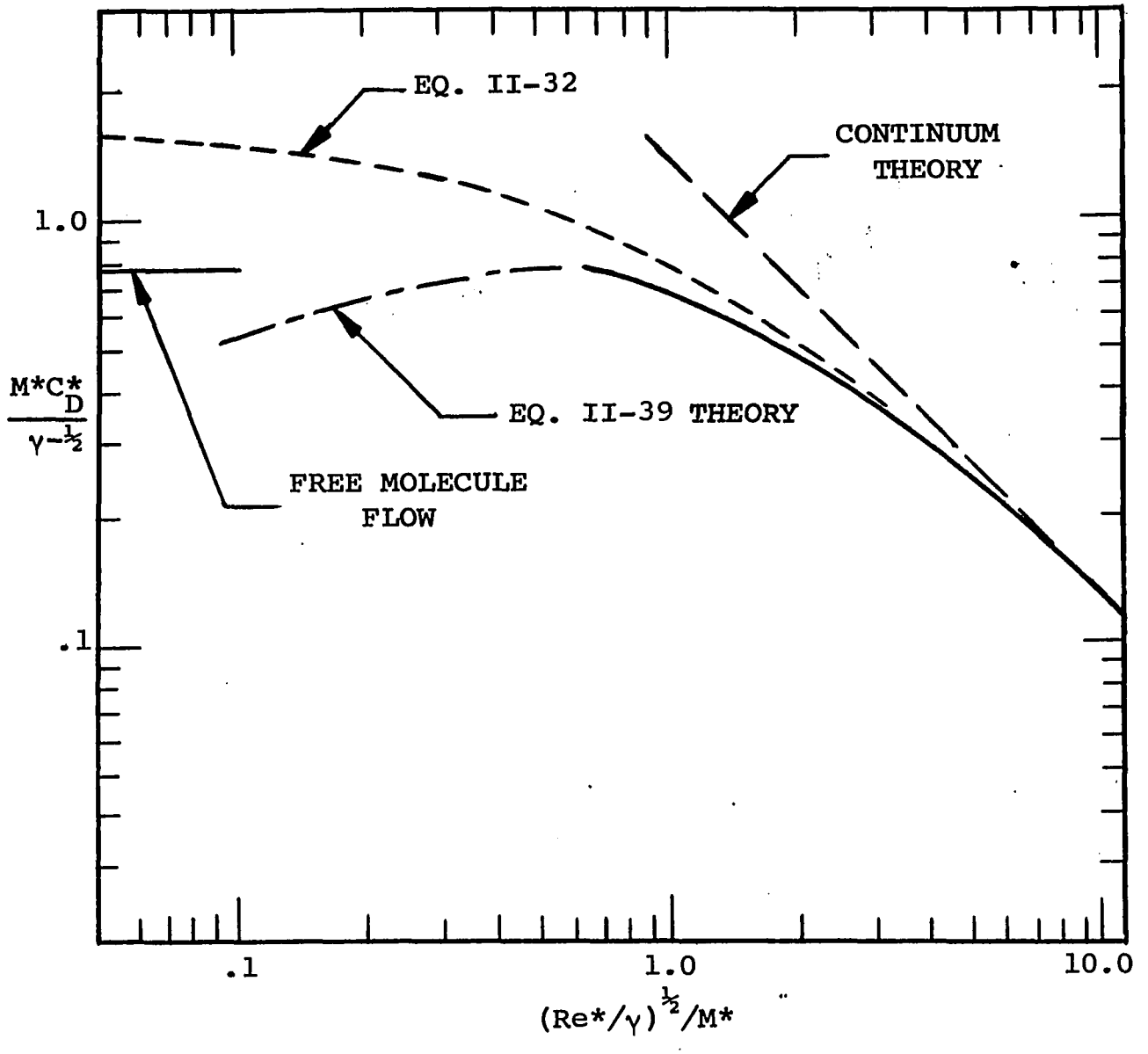

FIGURE II-2 DRAG COEFFICIENT OF A FLAT PLATE

Table II-1 Values of $\eta_{\mathcal{H}}$ versus $(Re^*/\gamma)^{\frac{1}{2}}/M^*$

$(Re^*/\gamma)^{\frac{1}{2}}/M^*$	$\eta_{\mathcal{H}}$
0.00771	2.0
0.01132	1.9
0.01655	1.8
0.0236	1.7
0.0331	1.6
0.0454	1.5
0.0616	1.4
0.0825	1.3
0.1086	1.2
0.1412	1.1
0.1818	1.0
0.232	0.9
0.296	0.8
0.376	0.7
0.481	0.6
0.622	0.5
0.828	0.4
1.160	0.3
1.796	0.2
3.680	0.1
36.80	0.01

Substitution of Equation II-33 into II-29 gives for the skin friction

$$(\gamma)^{\frac{1}{2}} M^* c_F^* = 0.664\, e^{-\eta_\mu^2} M^* \left(\frac{\gamma}{Re^*}\right)^{\frac{1}{2}} \qquad \text{(II-36)}$$

This equation is plotted in Figure II-1 along with Equation II-30.

An expression for the average drag coefficient can be obtained by using Equation II-35 for the skin friction coefficient

$$C_D^* = \frac{1}{L} \int_{\infty}^{\eta_{\mu_L}} c_F^* \frac{dx}{d\eta}\, d\eta \qquad \text{(II-37)}$$

In this integration, ψ, defined by Equations II-8 and II-9, is a constant since as $\eta \to \eta_\mu$, ψ must approach the value ψ_μ at any x. This therefore, gives

$$\frac{\partial \psi_\mu}{\partial x} = -2.888 \frac{\rho_\mu v_\mu}{\rho_\infty U} \qquad \text{(II-38)}$$

Since $v_\mu = 0$ by definition, then $\partial \psi_\mu / \partial x = 0$ which makes, upon integration, Equation II-37,

$$(\gamma)^{\frac{1}{2}} M^* C_D^* = 1.328 \left\{ \eta_{\mu_L} M^* \left(\frac{\gamma}{Re^*}\right)^{\frac{1}{2}} \right\} \cdot \left\{ \frac{1}{\eta_{\mu_L} \exp(\eta_{\mu_L}^2)} - 1.772\, \mathrm{erfc}(\eta_{\mu_L}) \right\} \qquad \text{(II-39)}$$

Equation II-39 is plotted in Figure II-2 along with Equation II-32.

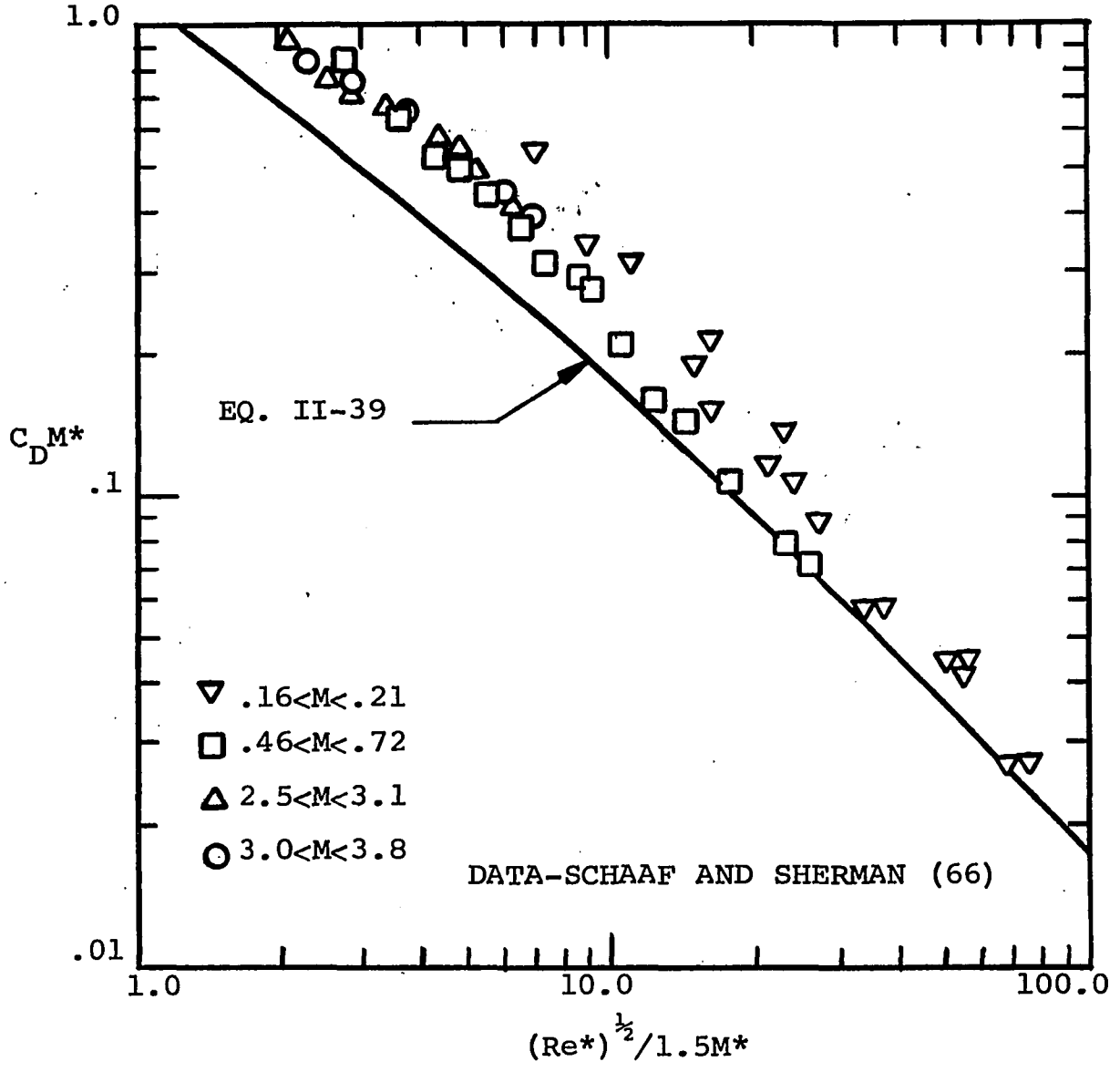

FIGURE II-3 COMPARISON OF FLAT PLATE DRAG COEFFICIENT WITH DATA OF SCHAAF AND SHERMAN

CHAPTER III

INTERNAL FLOW

This chapter concerns itself with the flow of rarefied gases in internal flow geometries (e.g. inside tubes) which are of engineering interest, particularly in vacuum engineering. Industrial processes utilizing very low pressures which were rare twenty-five years ago are now commonplace. Vacuum furnaces in the metal industry, vacuum coating of microcircuits in the electronic industry, vacuum freeze-drying in the drug and other industries are but a few of the multitude of present applications of vacuum techniques. The intense interest in space exploration in recent years has also created a demand for an increased knowledge of flow processes under conditions of moderate to high vacuum.

Since the initial experiments of Hagen (32) in 1839 and Poiseuille (33) in 1840-41, extensive investigations of the flow of fluids through tubes have been carried on. The beginning of this century saw the analysis of gas flows through tubes extended to the region of very low pressures by the work of Knudsen (34), Maxwell (1), Gaede (35) and Smoluchowski (36). The limiting problems for infinitely long tubes have exact mathematical solutions with experimental verification in both continuum flow (37), and free molecule flow (38).

Much data have been presented for the intermediate range (2, 38,39,40,41,42), and several solutions have been developed from these data. Excellent summaries of the theoretical and experimental results for rarefied internal flows may be found in references 43, 44 and 45.

The classical problems of Couette and Poiseuille flows will be considered in this chapter, as well as the problems of flow through rectangular and triangular ducts.

A. Couette Flow

Couette flow is the name ascribed to the flow of fluid between two infinitely long and wide plates, one of which is at rest and the other is moving with a constant velocity in a direction parallel to the plate at rest. Numerous kinetic theory analyses of the problem can be found in references 46, 47, 48, 49, 50, 51 and 52. The defining continuum equation for this type of flow is the same as that for the Rayleigh problem; namely,

$$\frac{\partial u}{\partial t} = \nu \frac{\partial^2 u}{\partial y^2} \tag{III-1}$$

but with the appropriate continuum boundary conditions

$$\begin{aligned} u &= U \quad y = 0 \text{ and } t > 0 \\ u &= 0 \quad y = h \text{ and } t > 0 \end{aligned} \tag{III-2}$$

and the initial condition

$$u = 0 \quad 0 \leq y \leq h \text{ and } t = 0 \tag{III-3}$$

The solution of Equation III-1 which satisfies the boundary and initial conditions of Equations III-2 and III-3 can be obtained in the form of a series of complementary error functions (53)

$$u = U \sum_{n=0}^{\infty} \left\{ \operatorname{erfc}\left[\frac{nh}{(\nu t)^{\frac{1}{2}}} + \frac{y}{2(\nu t)^{\frac{1}{2}}} \right] - \operatorname{erfc}\left[\frac{(n+1)h}{(\nu t)^{\frac{1}{2}}} - \frac{y}{2(\nu t)^{\frac{1}{2}}} \right] \right\} \tag{III-4}$$

The limiting case (i.e. the steady-state value) for this series of functions is

$$u = -U\left[\frac{y}{h} - 1\right] \tag{III-5}$$

where U is the velocity of the moving plate, y is the coordinate measured normal to the plates, and h is the distance between the plates. Substitution of this equation into the equation for shear stress, (Equation II-24), leads to

$$\tau = \mu \frac{U}{h} \tag{III-6}$$

and the skin friction, (Equation II-29), becomes

$$c_F = \frac{2\mu}{\rho U h} \tag{III-7}$$

The parameter h, Figure III-1, must be replaced by the distance, h_1, between the plates in the slip flow Couette problem. The relation between these two distances can be evaluated as

$$\begin{aligned} h &= h_1 + 2\lambda \frac{2-\sigma}{\sigma} \\ &= h_1\left(1 + 2 \frac{\lambda}{h_1} \frac{2-\sigma}{\sigma}\right) \end{aligned} \qquad \text{(III-8)}$$

Notice that when the mean free path, λ, is small, which corresponds to small slip velocities, h approaches h_1. This is to be expected since for negligible slip the continuum and the slipping plates should coincide, which will be the case if $h = h_1$. Introducting Equation III-8 into III-7 gives

$$\begin{aligned} c_F &= \frac{2\mu}{\rho U h_1\left(1 + 2 \frac{\lambda}{h_1} \frac{2-\sigma}{\sigma}\right)} \\ &= \frac{2}{Re\left(1 + 2 \frac{\lambda}{h_1} \frac{2-\sigma}{\sigma}\right)} \end{aligned} \qquad \text{(III-9)}$$

where $Re = \rho U h_1/\mu$. The term λ/h_1 may be replaced by its equivalent expression (i.e., Equation I-4); thus

$$c_F = \frac{2}{Re} \frac{1}{\left[1 + 2.52(\gamma)^{\frac{1}{2}} \left(\frac{2-\sigma}{\sigma}\right) \frac{M}{Re}\right]} \qquad \text{(III-10)}$$

The continuum limit (i.e., $M/Re \to 0$) for this expression is 2/Re which is the accepted value predicted by continuum theory. Also, the free molecule limit (i.e., $M/Re \to \infty$) for Equation III-10 is

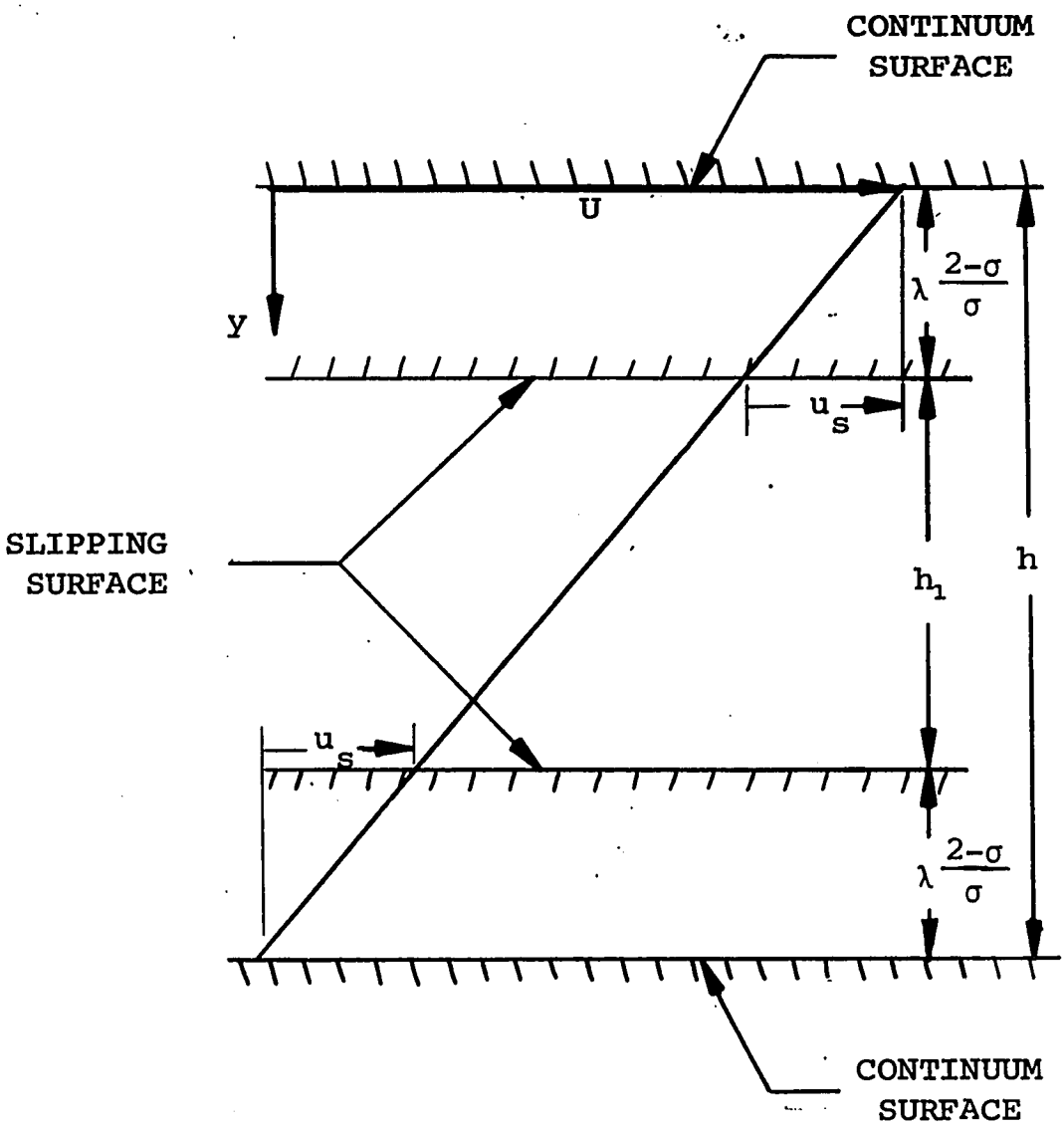

FIGURE III-1 SUPERPOSITION OF SLIPPING AND NONSLIPPING PLATES FOR COUETTE FLOW

$$Mc_F \rightarrow \frac{0.798\sigma}{(\gamma)^{\frac{1}{2}}(2-\sigma)} \qquad \text{(III-11)}$$

which is the correct value (5) for free molecule flow.

Equation III-10 is the same as that derived by Millikan (15) using the conventional approach of solving Equation III-1 with a slip velocity boundary condition. Equation III-10 is plotted in Figure III-2.

B. Poiseuille Flow

The fully established steady laminar flow through a circular tube of radius R is a special case of parallel flow with rotational symmetry. The governing continuum equations for this type of flow are again the continuity and Navier-Stokes equations. To facilitate the analysis these equations are given in cylindrical coordinates. The continuity equation is

$$\frac{\partial v_r}{\partial r} + \frac{v_r}{r} + \frac{1}{r}\frac{\partial v_\varphi}{\partial \varphi} + \frac{\partial v_z}{\partial z} = 0 \qquad \text{(III-12)}$$

and the Navier-Stokes equation in three component directions, (r, φ, z), are, respectively,

$$\rho\left(v_r \frac{\partial v_r}{\partial r} + \frac{v_\varphi}{r}\frac{\partial v_r}{\partial \varphi} - \frac{v_\varphi^2}{r} + v_z \frac{\partial v_r}{\partial z}\right) =$$

$$-\frac{\partial p}{\partial r} + \mu\left(\frac{\partial^2 v_r}{\partial r^2} + \frac{1}{r}\frac{\partial v_r}{\partial r} - \frac{v_r}{r^2} + \frac{1}{r^2}\frac{\partial^2 v_r}{\partial \varphi^2} - \frac{2}{r^2}\frac{\partial v_\varphi}{\partial \varphi} + \frac{\partial^2 v_r}{\partial z^2}\right) \qquad \text{(III-13)}$$

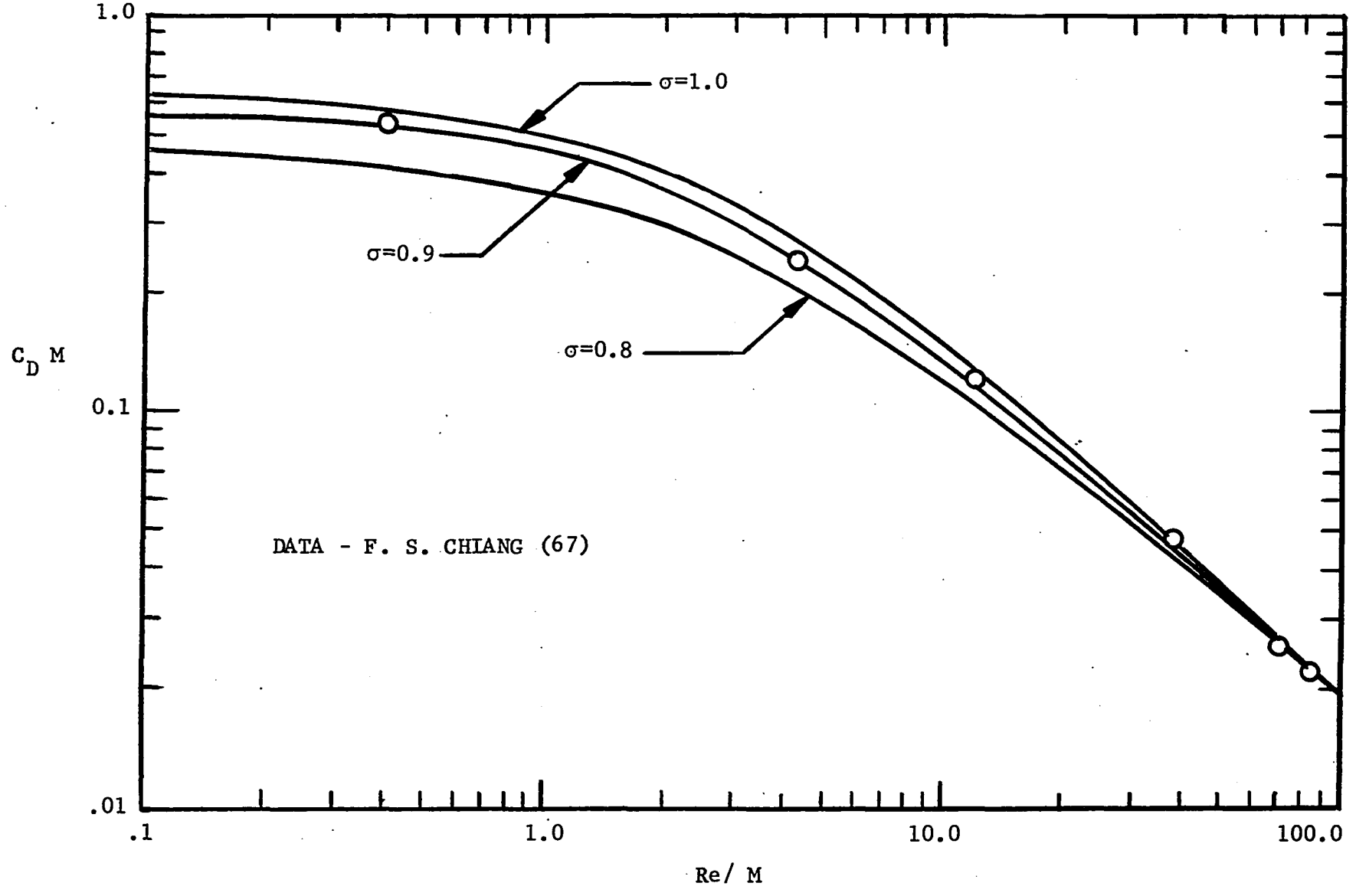

FIGURE III-2 COMPARISON OF DRAG COEFFICIENT FOR COUETTE FLOW WITH DATA OF F. S. CHIANG

$$\rho\left(v_r \frac{\partial v_\varphi}{\partial r} + \frac{v_\varphi}{r}\frac{\partial v_\varphi}{\partial \varphi} + \frac{v_r v_\varphi}{r} + v_z \frac{\partial v_\varphi}{\partial z}\right) =$$

$$- \frac{1}{r}\frac{\partial p}{\partial \varphi} + \mu\left(\frac{\partial^2 v_\varphi}{\partial r^2} + \frac{1}{r}\frac{\partial v_\varphi}{\partial r} - \frac{v_\varphi}{r^2} + \frac{1}{r^2}\frac{\partial^2 v_\varphi}{\partial \varphi^2} + \frac{2}{r^2}\frac{\partial v_r}{\partial \varphi} + \frac{\partial^2 v_\varphi}{\partial z^2}\right) \qquad \text{(III-14)}$$

$$\rho\left(v_r \frac{\partial v_z}{\partial r} + \frac{v_\varphi}{r}\frac{\partial v_z}{\partial \varphi} + v_z \frac{\partial v_z}{\partial z}\right) = - \frac{\partial p}{\partial z}$$

$$+ \mu\left(\frac{\partial^2 v_z}{\partial r^2} + \frac{1}{r}\frac{\partial v_z}{\partial r} + \frac{1}{r^2}\frac{\partial^2 v_z}{\partial \varphi^2} + \frac{\partial^2 v_z}{\partial z^2}\right) \qquad \text{(III-15)}$$

where steady state and zero body forces are assumed.

A flow is called parallel if only the velocity component along the directions of the axis of symmetry, v_z, is different from zero, (i.e., all fluid particles moving in one direction). Thus if the radial, v_r, and angular, v_φ, components of the velocity are zero everywhere, it follows at once from the equation of continuity, (III-12), that $\partial v_z/\partial z = 0$, which means that the velocity in the flow direction is uniform with respect to z. Also since the flow is symmetrical, v_z, will not be a function of the angle, φ. Thus for this type of flow one obtains

$$v_z = v_z(r) \qquad v_\varphi \equiv 0 \qquad v_r \equiv 0 \qquad \text{(III-16)}$$

Further, it follows from the Navier-Stokes equations, (III-13 and III-14), that $\partial p/\partial r = 0$, and $\partial p/\partial \varphi = 0$, so that the

pressure depends only on z. Thus of the three components of the Navier-Stokes equations, only the one for the axial direction, z, remains, and it simplifies to

$$\mu\left(\frac{d^2v_z}{dr^2} + \frac{1}{r}\frac{dv_z}{dr}\right) = \frac{dp}{dz} \qquad \text{(III-17)}$$

where the z axis corresponds to the axis of the tube, and r denotes the radial coordinate measured from the axis outward. The pressure gradient is constant along the tube. This is the defining equation for Poiseuille flow through a pipe.

The solution of Equation III-17 with the boundary condition $v_z = 0$ at $r = R$ gives the velocity distribution, namely

$$v_z = -\frac{1}{4\mu}\frac{dp}{dz}(R^2 - r^2) \qquad \text{(III-18)}$$

An expression for the mean velocity, U, may be developed by evaluation of the following integral

$$U = \frac{1}{A}\int_0^R v_z dA \qquad \text{(III-19)}$$

where A is the cross section area of the tube and R is the radius of the tube. Substituting Equation III-18 into III-19 and integrating gives

$$U = -\frac{R^2}{8\mu}\frac{dp}{dz} \qquad \text{(III-20)}$$

The distance between the slipping and non-slipping tubes (Figure III-3) can be calculated using Equation III-18. The

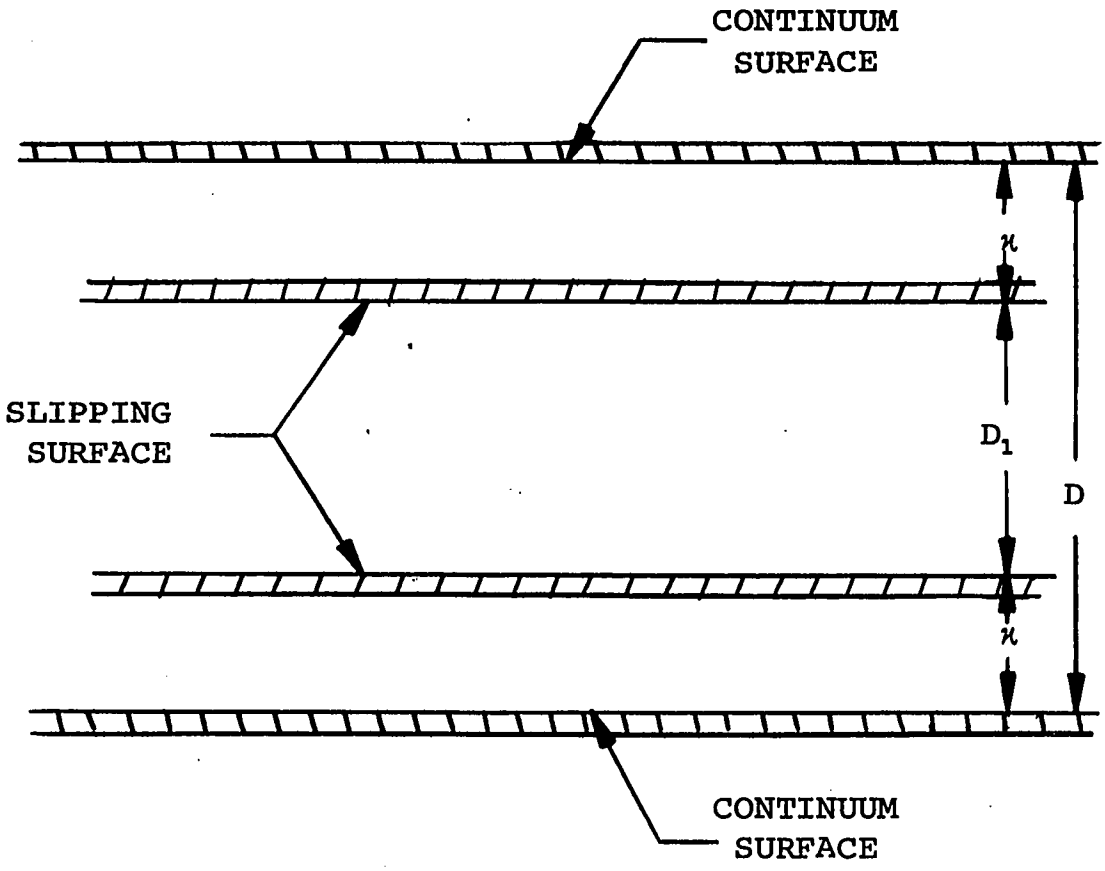

FIGURE III-3 SUPERPOSITION OF SLIPPING AND NONSLIPPING PIPES FOR POISEUILLE FLOW

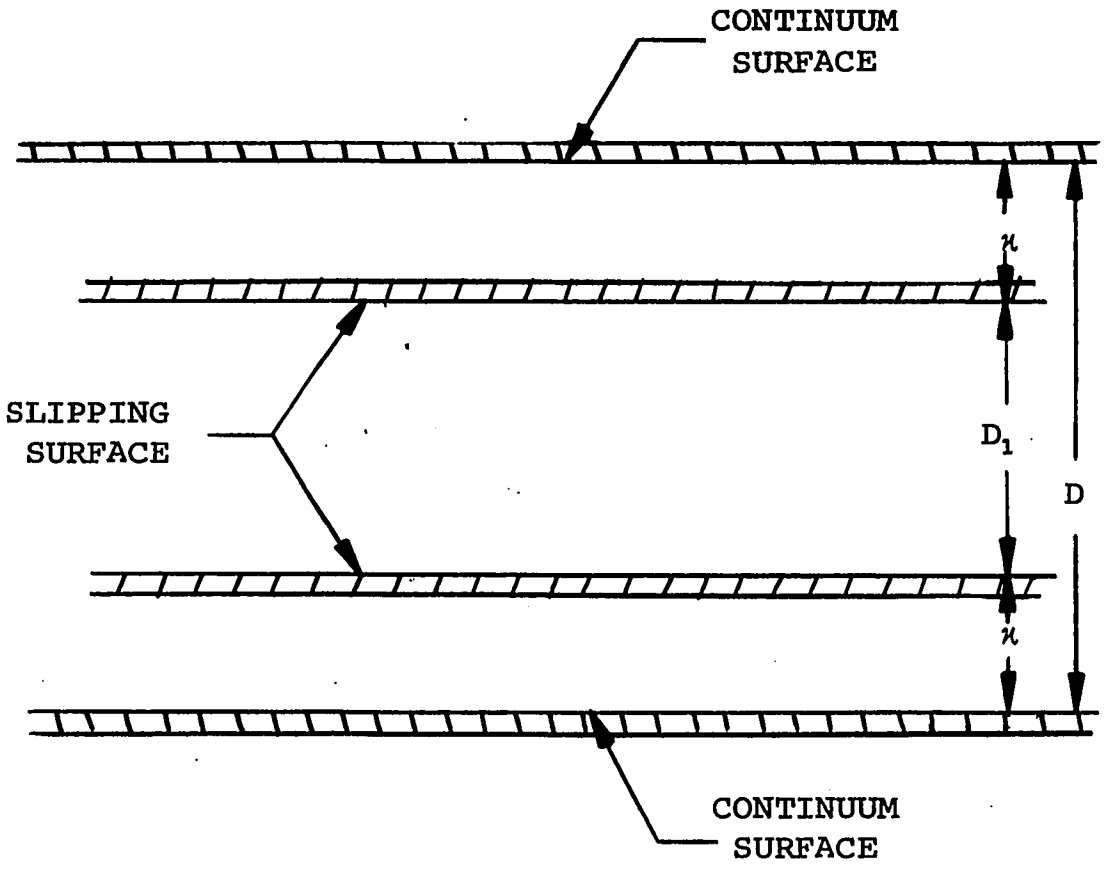

FIGURE III-3 SUPERPOSITION OF SLIPPING AND NONSLIPPING PIPES FOR POISEUILLE FLOW

slip velocity, v_s, will occur at R_1, hence,

$$v_s = v_z(R_1) = - \frac{1}{4\mu} \frac{dp}{dz} (R^2 - R_1^2) \qquad \text{(III-21)}$$

However, from Equation II-2, the slip velocity now becomes

$$v_s = - \frac{2-\sigma}{\sigma} \lambda \frac{dv_z}{dr} \Big)_{r = R_1} \qquad \text{(III-22)}$$

where the minus sign is due to the fact that dr is positive in the radially outward direction; whereas the ∂y in the defining equation for the slip velocity (II-2) is measured from the surface outward. Substitution of Equation III-18 into III-22 gives

$$v_s = - \frac{2-\sigma}{\sigma} \lambda \frac{1}{2\mu} \frac{dp}{dz} R_1 \qquad \text{(III-23)}$$

Equating Equations III-21 and III-23 leads to

$$R = \left(R_1^2 + 2R_1 \frac{2-\sigma}{\sigma} \lambda\right)^{\frac{1}{2}} \qquad \text{(III-24)}$$

The separation distance, $\varkappa$, is simply the difference of the radii of the two tubes (i.e., $\varkappa = R_1 - R$). It should be noted that R_1 is a constant defined by actual tube radius, and R is a variable which depends upon the degree of slip. The mean free path, λ, may be replaced in Equation III-24 by its equivalent expression, $\lambda = 2R_1K$, where K is the Knudsen number; hence

$$R = R_1\left(1 + 4 \frac{2-\sigma}{\sigma} K\right)^{\frac{1}{2}} \qquad \text{(III-25)}$$

Equation III-25 may be used to eliminate R from Equation III-20, hence

$$U = - \frac{R_1^2}{8\mu} \frac{dp}{dz} \left(1 + 4 \frac{2-\sigma}{\sigma} K\right) \qquad \text{(III-26)}$$

The pressure drop correction coefficient, φ, is defined as

$$\varphi = - \frac{32\mu U}{D_1^2} \frac{1}{\frac{dp}{dz}} \qquad \text{(III-27)}$$

Using Equation III-26 to eliminate the pressure gradient leads to, after simplification,

$$\varphi = 1 + 4 \frac{2-\sigma}{\sigma} K \qquad \text{(III-28)}$$

Maxwell (1) gives the following expression for the pressure drop coefficient

$$\varphi = 1 + 8 \frac{2-\sigma}{\sigma} K \qquad \text{(III-29)}$$

Maxwell's analysis, as in all cases, is based on a solution of Equation III-17 with a slip boundary condition.

Equation III-28 is presented in Figure III-4.

C. Flow Through Rectangular Duct

The flow field for this configuration is the same a s for Poiseuille flow (i.e., parallel flow - all particles moving in one direction). Thus since the v and w components

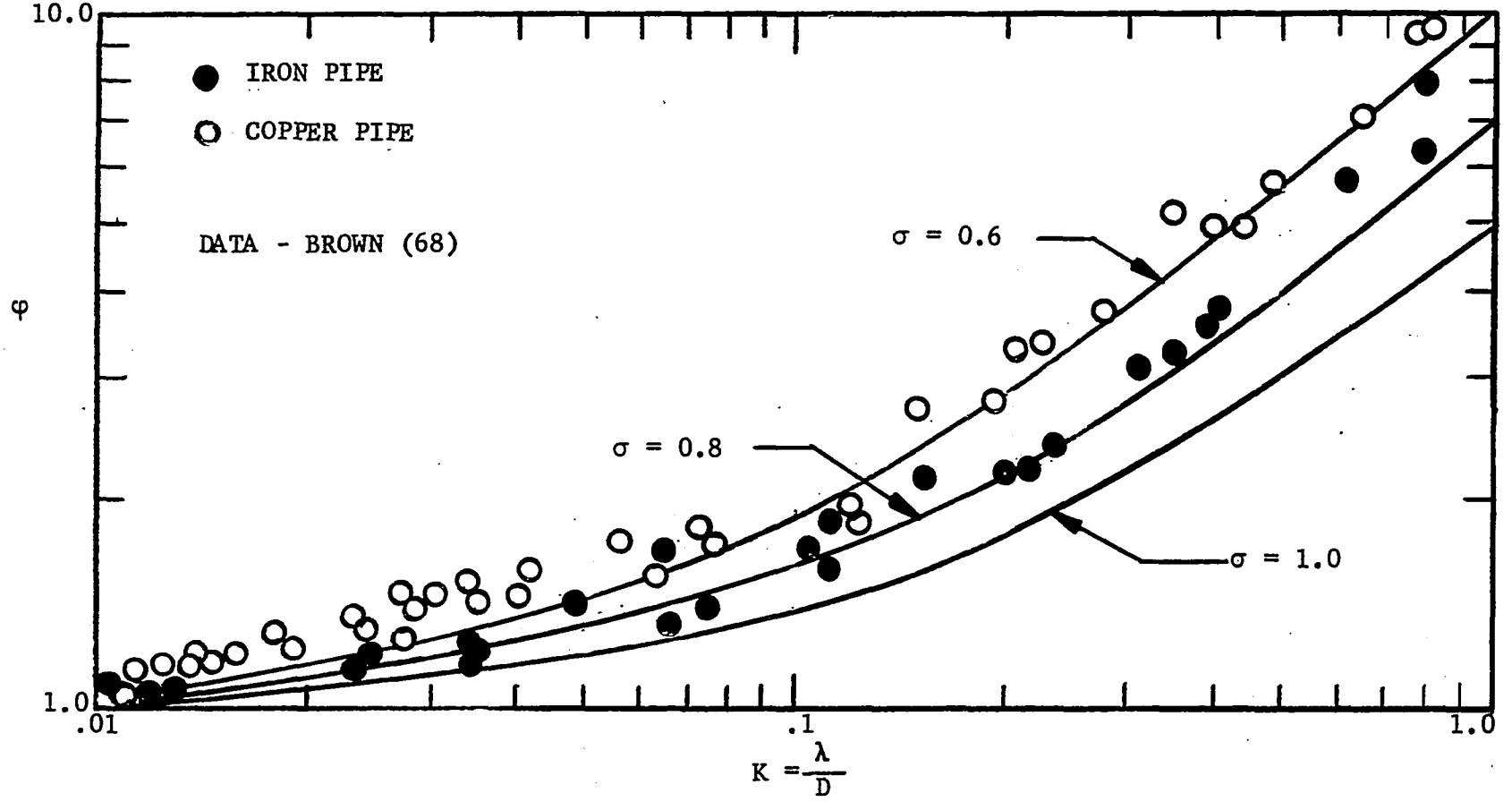

FIGURE III-4 COMPARISON OF PRESSURE DROP CORRECTION COEFFICIENT FOR POISEUILLE FLOW WITH DATA OF BROWN, ET AL

of the velocity are zero the Navier-Stokes equations will reduce to

$$\frac{\partial^2 u}{\partial y^2} + \frac{\partial^2 u}{\partial z^2} = \frac{1}{\rho\mu}\frac{dp}{dx} \qquad \text{(III-30)}$$

where the x direction is taken along the axis of the duct, the y and z axes are taken to be parallel to the sides, and the origin of the coordinate system is taken at the corner (Figure III-5). Again, as in Poiseuille flow, the pressure gradient is constant.

For a duct of rectangular cross section with sides a and b in the directions y and z respectively, the foregoing equation is satisfied by (Appendix A)

$$u = \frac{1}{2\rho\mu}\frac{dp}{dx}(y-a)y + \sum_{m=1}^{\infty} \sin\frac{m\pi y}{a}(\cos m\pi - 1)\frac{2a^2}{\rho\mu m^3\pi^3}\frac{dp}{dx}\left[\frac{\sinh\frac{m\pi z}{a}}{\sinh mn\pi}(\cosh mn\pi - 1) - \cosh\frac{m\pi z}{a}\right] \qquad \text{(III-31)}$$

where $n = b/a$.

The separation distance, $\varkappa$, (Figure III-6) may now be calculated by matching this velocity to its equivalent slip velocity, at $z = \varkappa$,

$$u(\varkappa) = \lambda\frac{\partial u}{\partial z}\Big)_{z=\varkappa} \qquad \text{(III-32)}$$

where σ has been assumed to be equal to unity for simplicity.

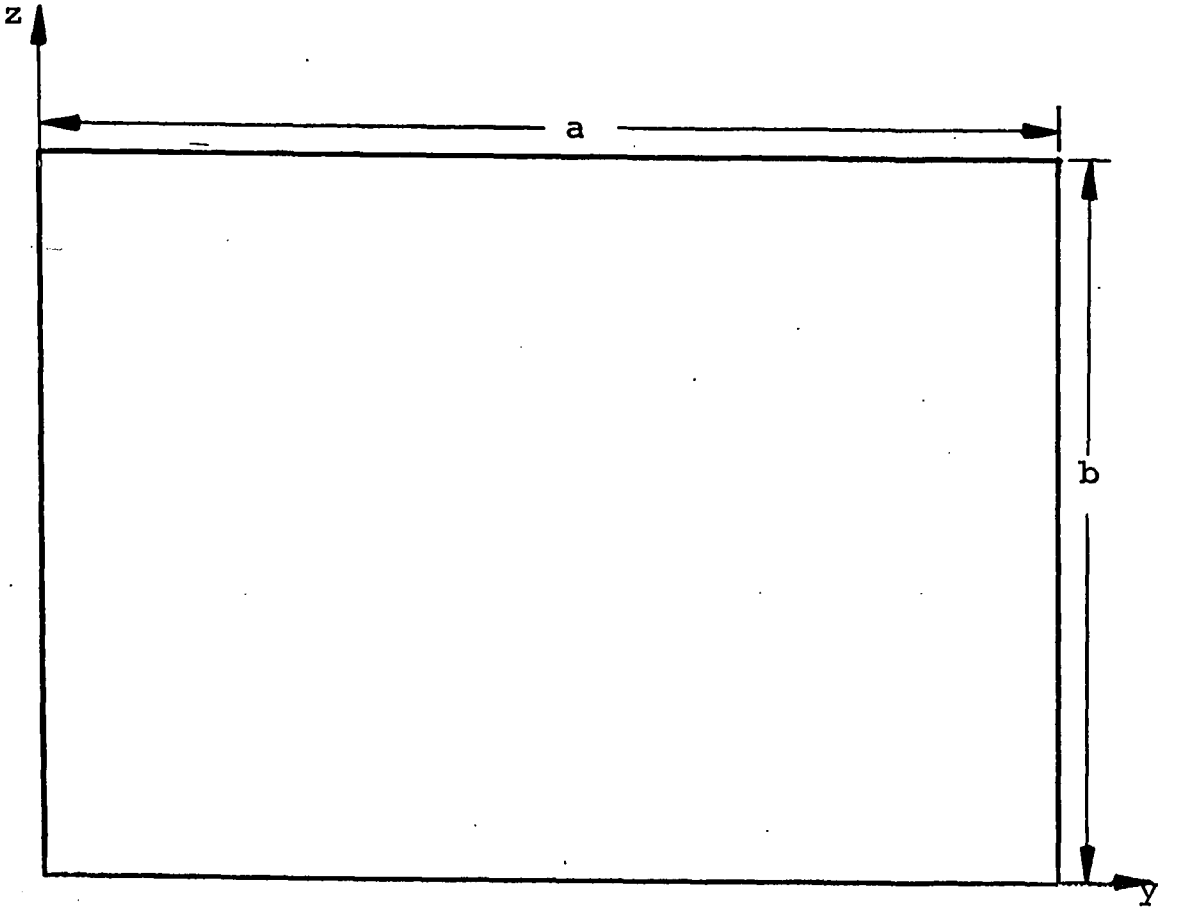

FIGURE III-5 CROSS SECTION OF RECTANGULAR DUCT SHOWING COORDINATE AXES

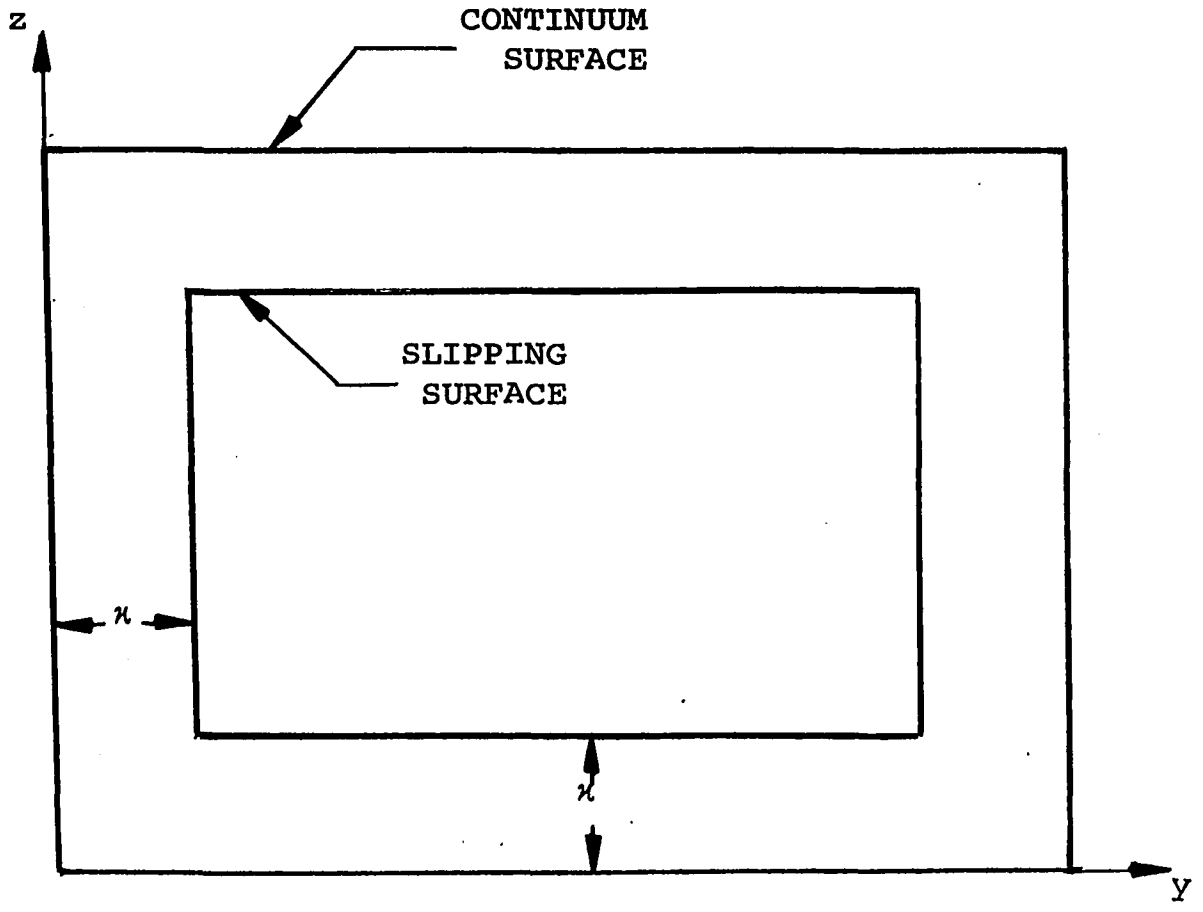

FIGURE III-6 SUPERPOSITION OF SLIPPING AND NONSLIPPING RECTANGULAR DUCTS

Substituting Equation III-31 into III-32 yields the following implicit expression for $\varkappa$

$$\frac{1}{2\rho\mu}\frac{dp}{dx}(y-a)y + \sum_{m=1}^{\infty}\sin\frac{m\pi y}{a}(\cos m\pi - 1)\frac{2a^2}{\rho\mu m^3\pi^3}\frac{dp}{dx} \cdot$$

$$\left[\frac{\sinh\frac{m\pi\varkappa}{a}}{\sinh mn\pi}(\cosh mn\pi - 1) - \cosh\frac{m\pi\varkappa}{a}\right] = \lambda\sum_{m=1}^{\infty}\sin\frac{m\pi y}{a}(\cos m\pi - 1)$$

$$\frac{1}{\pi^2}\frac{2a}{\rho\mu m^2}\frac{dp}{dx}\left[\frac{\cosh\frac{m\pi\varkappa}{a}}{\sinh m\pi a}(\cosh mn\pi - 1) - \sinh\frac{m\pi\varkappa}{a}\right] \qquad \text{(III-33)}$$

Numerical values of $\varkappa$ can be obtained for various values of λ by use of a digital computer.

The average velocity, U, may be determined by the following integration

$$U = \frac{1}{A}\int_0^a\int_0^b u\, dzdy \qquad \text{(III-34)}$$

Substituting Equation III-31 into III-34 and integrating gives

$$U = -\frac{a^2}{2\rho\mu}\frac{dp}{dx}\left\{.167 + \frac{.129}{n}\sum_{m=1}^{\infty}\frac{(\cosh m\pi - 1)^2}{m^5} \cdot \left[\frac{(\cosh mn\pi - 1)^2}{\sinh mn\pi} - \sinh mn\pi\right]\right\} \qquad \text{(III-35)}$$

The pressure drop coefficient, Λ, is defined as

$$\Lambda = -\frac{2A}{\rho u^2}\frac{dp}{dx} \qquad \text{(III-36)}$$

where A is the cross sectional area of the real duct (i.e., the interior duct shown in Figure III-6). For the rectangular duct shown

$$\Lambda = - \frac{2(a-2\varkappa)(b-2\varkappa)}{\rho U^2} \frac{dp}{dx} \qquad \text{(III-37)}$$

The pressure gradient may be eliminated by using Equation III-35.

The parameter, Λ, will not be shown graphically since there is no applicable experimental data for this type of rarefied flow.

D. Flow Through Triangular Duct

Flow through a duct of triangular cross section may be analyzed by again solving the Navier-Stokes equation for parallel flow, Equation III-30. If the cross section is an equilateral triangle with sides of length b, and if the origin is taken at the geometric center of the cross section and the y-axis is taken to be parallel to one of the sides, (Figure III-7) the solution to Equation III-30 with constant pressure gradient is (see Appendix B)

$$u = - \frac{.29}{\rho \mu b} \frac{dp}{dx} (z + .289b)(z + 1.73y - .577b) \cdot (z - 1.73y - .577b) \qquad \text{(III-38)}$$

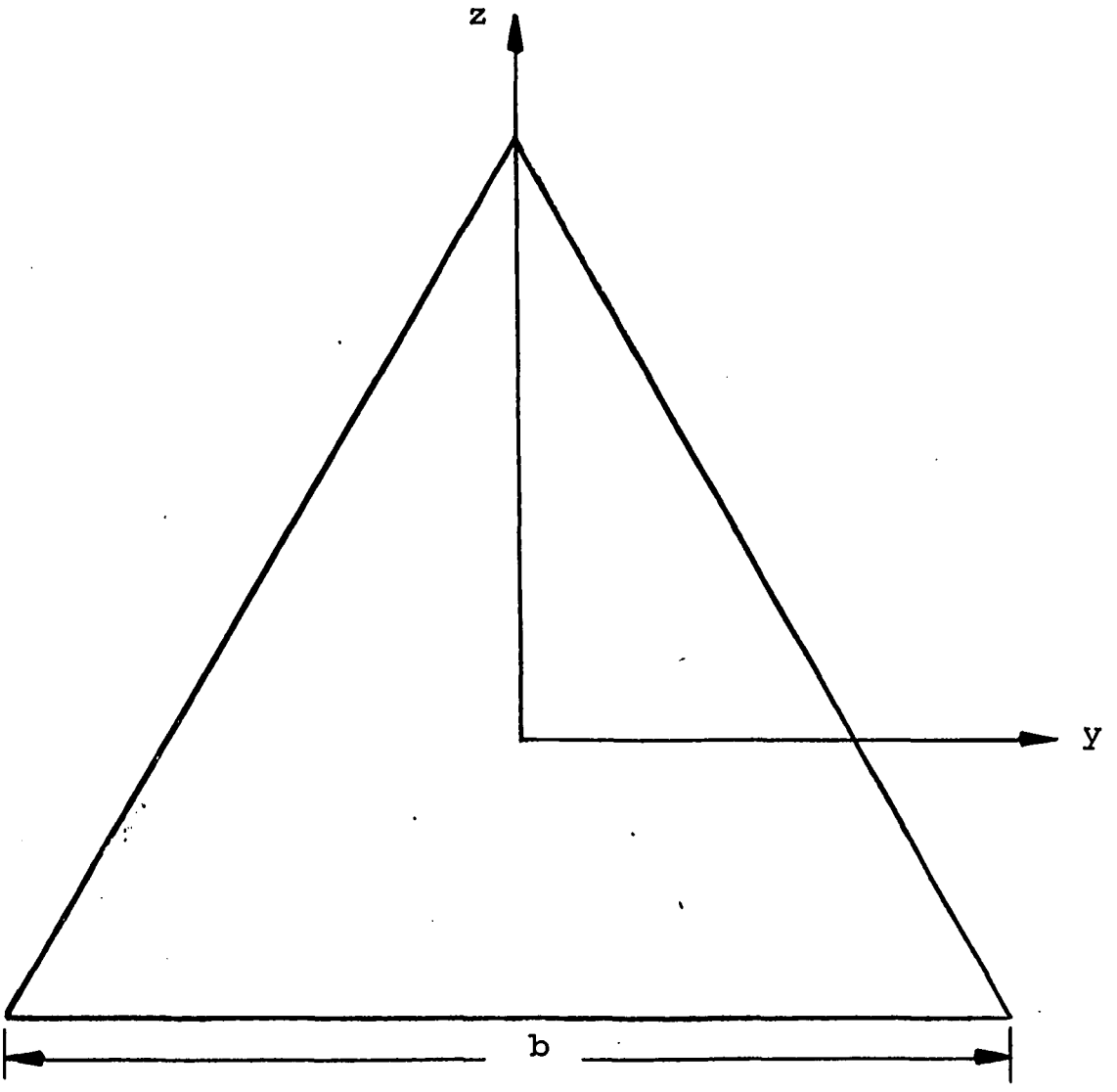

FIGURE III-7 CROSS SECTION OF TRIANGULAR DUCT SHOWING COORDINATE AXES

To calculate the separation distance, $\varkappa$, (Figure III-8) this velocity must be matched to its equivalent slip velocity as given by

$$u(\varkappa) = \lambda \left(\frac{\partial u}{\partial z}\right)_{z = z_{\varkappa},\ y = \text{constant}} \tag{III-39}$$

Substituting Equation III-38 into III-39 yields the following cubic equation

$$z_{\varkappa}^3 - .866bz_{\varkappa}^2 - (1.73b\lambda+3y^2)z_{\varkappa}+.096-(3\lambda+.866b)y^2 = 0 \tag{III-40}$$

The parameter $z_{\varkappa}$ will be constant for any value of y (see Figure III-8); therefore choosing y = 0, for ease of computation, Equation III-40 reduces to

$$z_{\varkappa}^3 - .866bz_{\varkappa}^2 - 1.73b\lambda z_{\varkappa} + .096 = 0 \tag{III-41}$$

The distance $z_{\varkappa}$ may now be evaluated as a function of the mean free path, λ, and is given as

$$\begin{aligned} z_{\varkappa} = .29b &+ \left\{-b^2(.024b-.25\lambda)+\left[b^4(.063\lambda^2-.012b\lambda+.006b^2)\right.\right. \\ &\left.\left. -b^3(.193\lambda^3+.083\lambda^2+.012\lambda+.0006)\right]^{\frac{1}{2}}\right\}^{1/3} \\ &+ \left\{-b^2(.024b-.25\lambda)-\left[b^4(.063\lambda^2-.012b\lambda+.006b^2)\right.\right. \\ &\left.\left. -b^3(.193\lambda^3+.083\lambda^2+.012\lambda+.0006)\right]^{\frac{1}{2}}\right\}^{1/3} \end{aligned} \tag{III-42}$$

From this equation the separation distance, $\varkappa(\varkappa = .29b + z_{\varkappa})$ can be calculated.

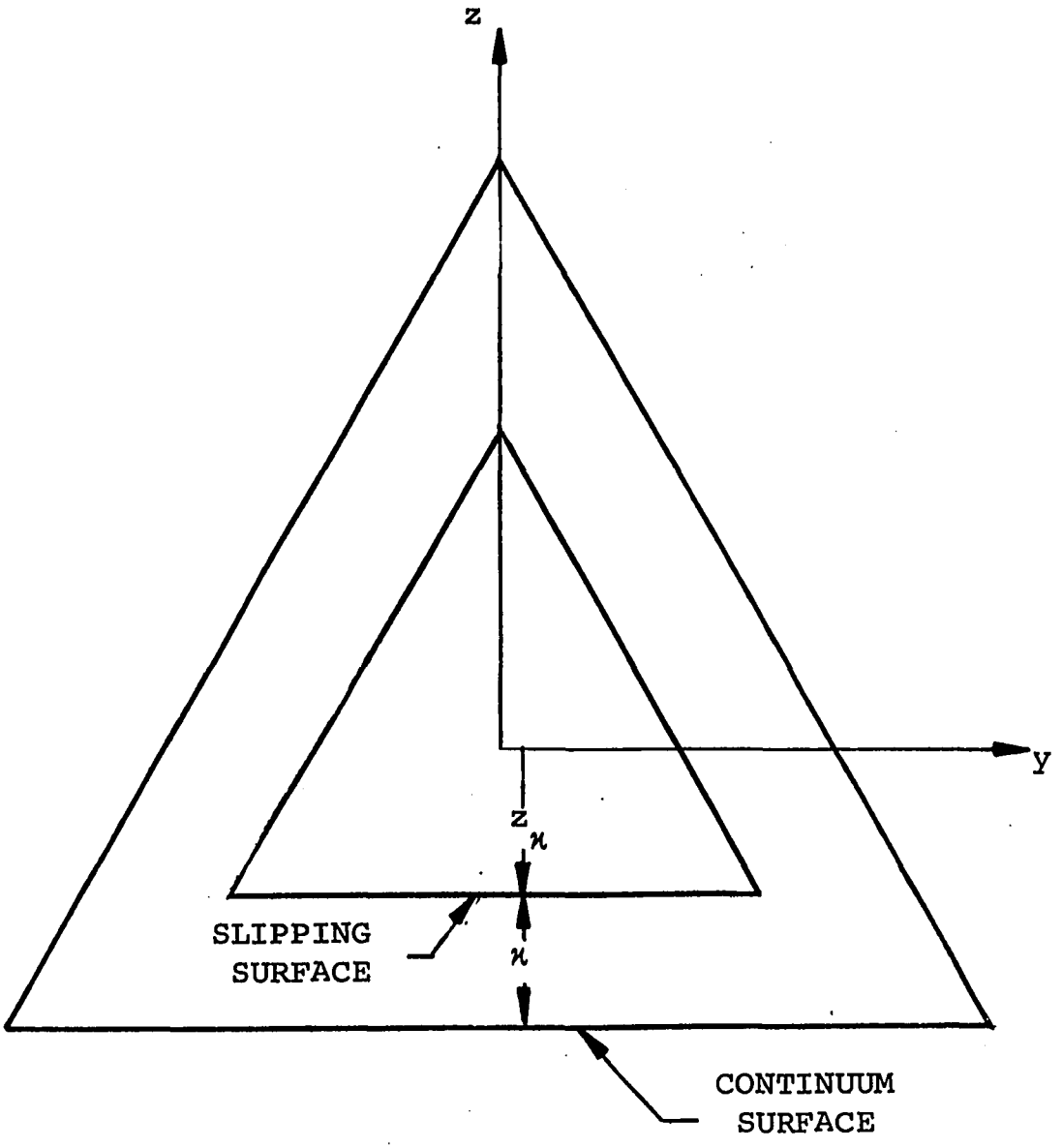

FIGURE III-8 SUPERPOSITION OF SLIPPING AND NONSLIPPING TRIANGULAR DUCTS

The average velocity, U, may be determined by the following integration

$$U = \frac{1}{A}\int_A u \, dA \qquad \text{(III-43)}$$

where u is given by Equation III-38. Since the flow is symmetrical the integral may be taken over one of the six symmetrical areas and then multiplied by six (Figure III-9), thus

$$U = \frac{13.8}{b^2}\int_0^{-.29b}\int_0^{-1.77z} u \, dydz \qquad \text{(III-44)}$$

Substituting Equation III-38 into III-44 and integrating gives

$$U = -\frac{.0078b^2}{\rho\mu}\frac{dp}{dx} \qquad \text{(III-45)}$$

For the triangular duct shown in Figures III-3 and III-9, the pressure drop coefficient, (Equation III-36) is given by

$$\Lambda = -\frac{41.6(.29b-\varkappa)^2}{\rho U^2}\frac{dp}{dx} \qquad \text{(III-46)}$$

The pressure gradient in Equation III-46 may be eliminated by use of Equation III-45; thus leading to

$$\Lambda = -5340\,\frac{\mu}{U}\left(.29 - \frac{\varkappa}{b}\right)^2 \qquad \text{(III-47)}$$

Again, as was the case for the rectangular duct, this parameter will not be depicted graphically due to lack of experimental data.

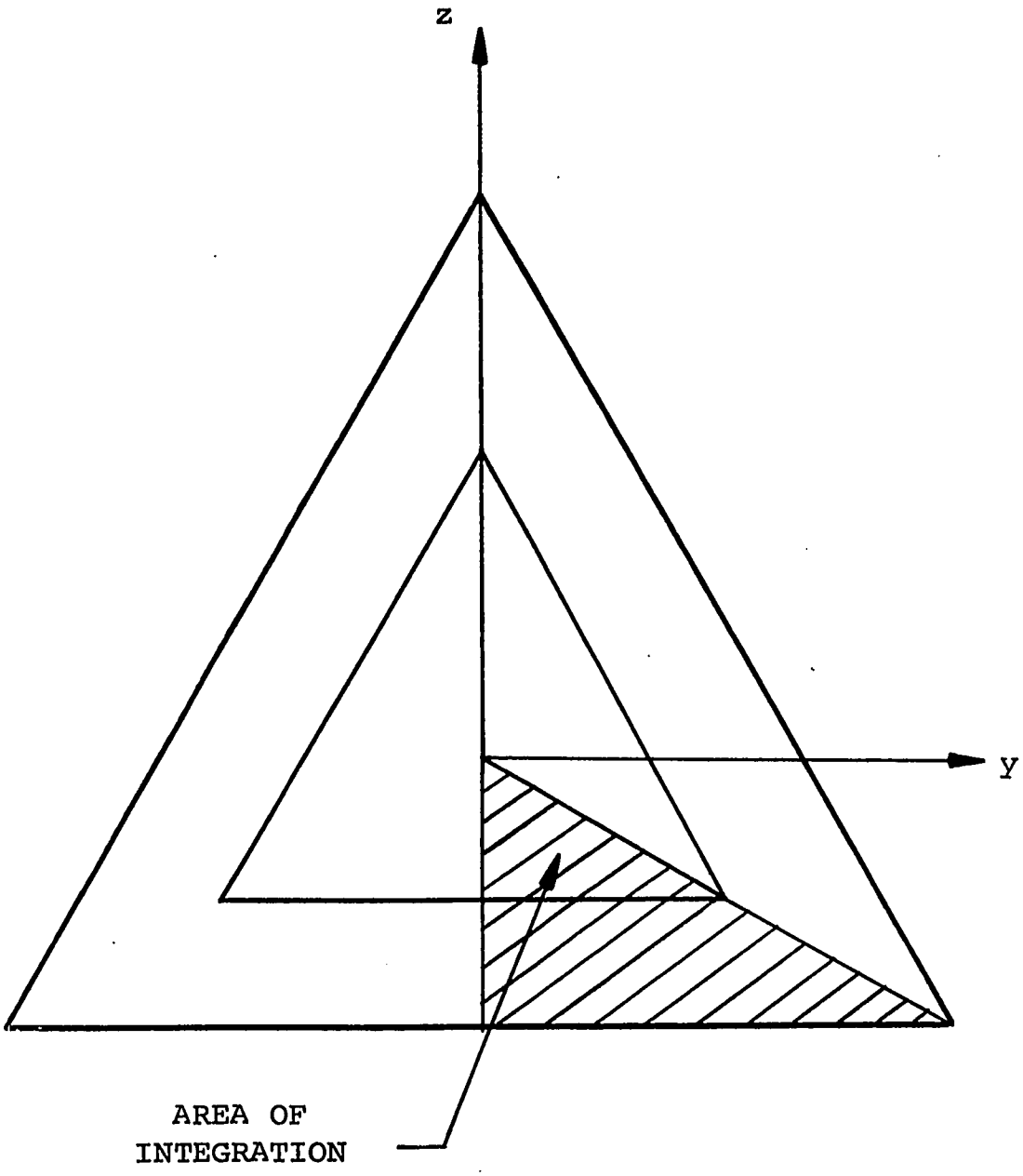

FIGURE III-9 CROSS SECTION OF TRIANGULAR DUCT SHOWING AREA OF INTEGRATION USED IN EQUATION III-43

CHAPTER IV

EXTERNAL FLOW

This chapter deals with the flow of a rarefied gas over an external surface (i.e., as opposed to flow inside tubes or between plates). Prior to World War II rarefied external flow problems were considered as a subject of academic interest rather than one of practical engineering importance. With the advent of rocketry, in the form of the V-2 rocket, the situation was radically changed and the possibility of high altitude, and corresponding low density, flights became a reality.

The configurations considered in this chapter are the cylinder and the wedge.

A. Flow Past a Right Circular Cylinder

The problem of flow around a right circular cylinder is formulated on the basis of Blasius' solution for flow past a cylinder. Other analyses have been carried out using modifications of the Navier-Stokes equations; for example, Lamb (54), Tsien's (2) unexplained "slight modification" of Lamb's work, and Tomotika and Aoi's (55) numerical solution of Oseen's perturbation of the Navier-Stokes equations. Analyses based on a kinetic theory

approach can be found in the works of Liu and Passamaneck (56), and Brooks and Reis (57).

The present analysis is based on the technique of introducing a fictitious nonslipping cylinder inside the actual slipping cylinder, but separated from it by a distance, $\varkappa$, that is proportional to the slip velocity (Figure IV-1).

The separation distance, $\varkappa$, between the cylinders is determined by equating the velocity, evaluated at $\varkappa$ to the slip velocity, Equation II-2; thus when the flow is of a continuum nature, the cylinders will coincide; but as the flow becomes rarefied the diameter of the fictitious cylinder will decrease.

By performing an order of magnitude analysis (53), as is customarily done in boundary layer problems, one can arrive at the simplified two dimensional Navier-Stokes equations given as

$$u \frac{\partial u}{\partial x} + v \frac{\partial u}{\partial y} = - \frac{1}{\rho} \frac{dp}{dx} + \nu \frac{\partial^2 u}{\partial y^2}$$

and the continuity equation

$$\frac{\partial u}{\partial x} + \frac{\partial v}{\partial y} = 0 \qquad \text{(IV-1)}$$

where u and v are the velocity components in the boundary layer and p is pressure. Steady state conditions and zero body forces have been assumed.

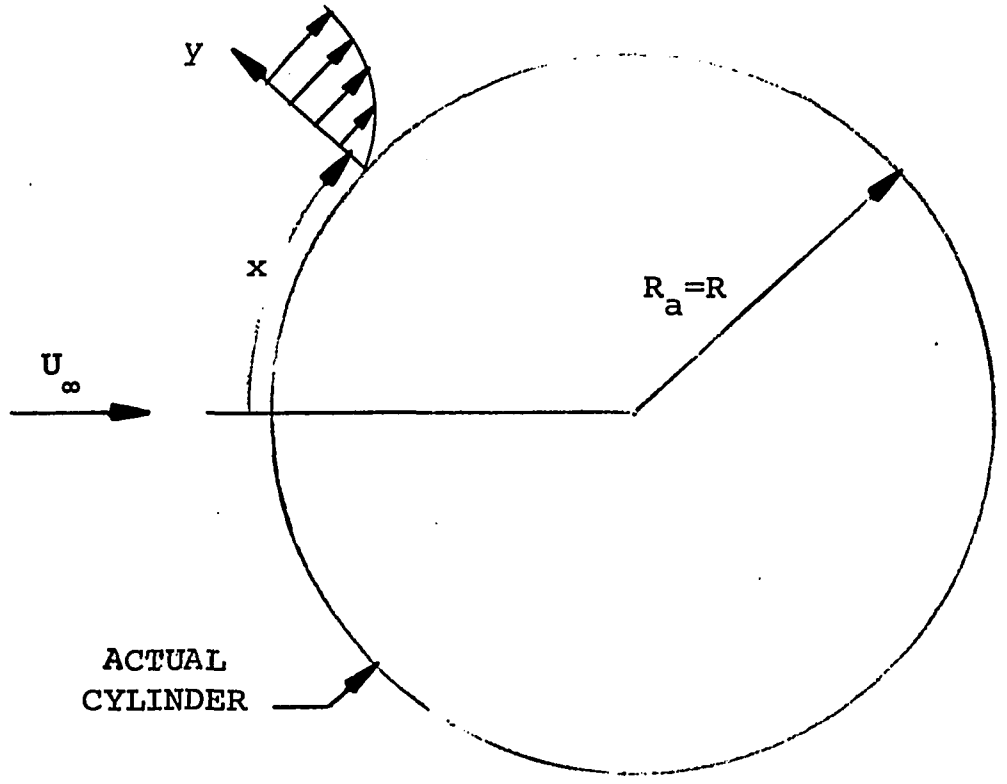

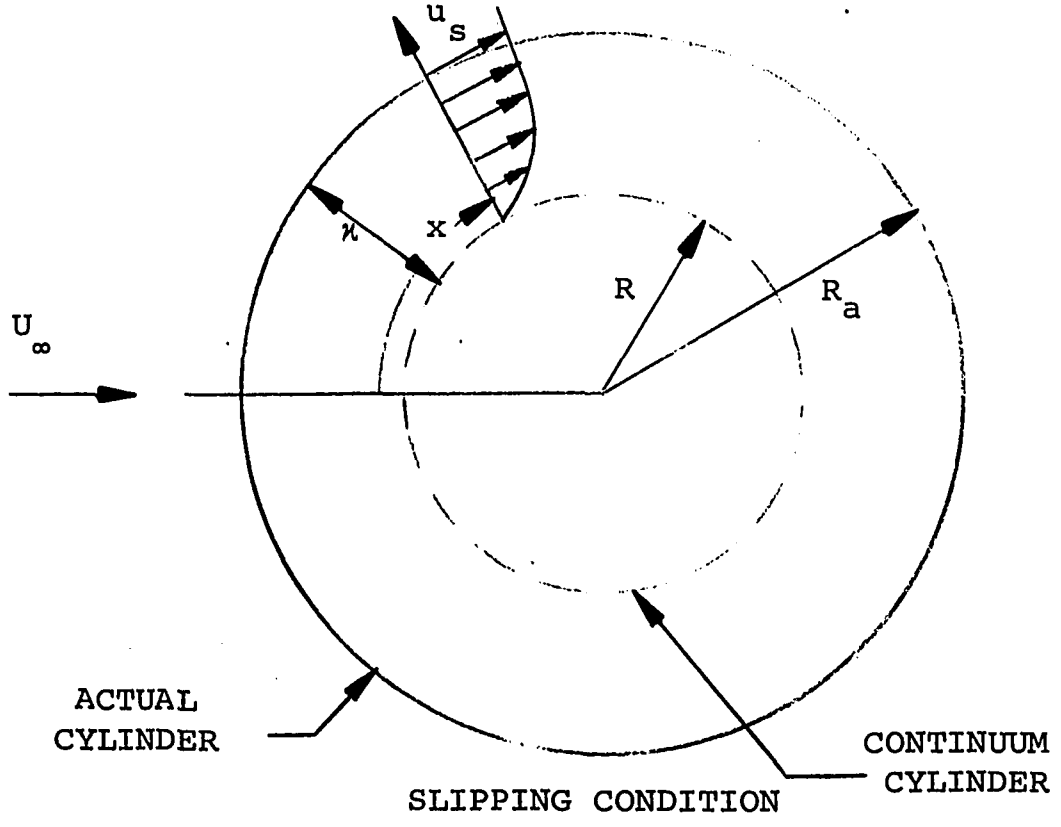

FIGURE IV-1 CYLINDER CROSS SECTION SHOWING COORDINATE REFERENCES AND ANGLES

The pressure gradient term in the simplified Navier-Stokes equation given above may be eliminated by the use of the Bernouilli equation

$$-\frac{1}{\rho}\frac{dp}{dx} = U\frac{dU}{dx}$$

where U is the potential flow velocity at the outer edge of the boundary layer. Upon substitution the defining Navier-Stokes equation becomes

$$u\frac{\partial u}{\partial x} + v\frac{\partial u}{\partial y} = U\frac{dU}{dx} + \nu\frac{\partial^2 u}{\partial y^2} \qquad \text{(IV-2)}$$

The boundary conditions are

$$\begin{aligned} y = 0 \quad & u = 0 \qquad v = 0 \\ y = \infty \quad & u = U(x) \end{aligned} \qquad \text{(IV-3)}$$

The potential flow velocity, U(x), is assumed to have the form of a power series in x where x denotes the distance from the stagnation point measured along the surface of the cylinder. The velocity profile in the boundary layer is also represented as a similar power series in x, where the coefficients are assumed to be functions of the coordinate y, measured at right angles to the wall (Blasius series). The general series for the potential flow velocity around a two dimensional surface is

$$U(x) = u_0 + u_1 x + u_2 x^2 + \ldots \qquad \text{(IV-4)}$$

where the coefficients u_0, u_1, ... depend only on the shape of the body and are known.

Blasius assumed the following series for the u and v component velocities

$$u = u_1 x f_1' + 4u_3 x^3 f_3' + 6u_5 x^5 f_5' + \ldots \qquad \text{(IV-5)}$$

and

$$v = -\left(\frac{\nu}{u_1}\right)^{\frac{1}{2}}\left[u_1 f_1 + \sum_{n=1}^{\infty}\left[(2n+2)(2n+1)u_{2n+1} x^{2n} f_{2n+1}\right]\right] \qquad \text{(IV-6)}$$

where the function coefficients f_1, f_3, ... are functions of $\eta = y(u_1/\nu)^{\frac{1}{2}}$, and the prime, $'$, denotes differentiation with respect to η. Inserting Equation IV-4, IV-5 and IV-6 into IV-2, and comparing terms, leads to a system of simultaneous ordinary differential equations for the functions f_1, f_3, ... the first two of which are

$$f_1'^2 - f_1 f_1'' = 1 + f_1''' \qquad \text{(IV-7)}$$

and

$$4f_1' f_3 - 3f_1'' f_e - f_1 f_3'' = 1 + f_3''' \qquad \text{(IV-8)}$$

All of the equations are ordinary differential equations of order three; however, Equation IV-7 is non-linear whose

solution will make the remaining equations linear. Tifford (58) has numerically calculated the functions f_1, f_3, ..., f_{11} along with their first and second derivatives.

The potential velocity for flow past a right circular cylinder of radius R and free stream velocity U_∞ is given (53) as

$$U(x) = 2U_\infty \sin\left(\frac{x}{R}\right) \qquad \text{(IV-9)}$$

If one writes the $\sin(x/R)$ term in a power series, Equation IV-9 becomes

$$U(x) = 2U_\infty\left[\frac{x}{R} - \frac{1}{3!}\left(\frac{x}{R}\right)^3 + \frac{1}{5!}\left(\frac{x}{R}\right)^5 - \ldots\right] \qquad \text{(IV-10)}$$

Comparison of Equations IV-10 and IV-4 leads to

$$u_0 = u_2 = u_4 = u_6 = u_8 = u_{10} = 0$$

$$u_1 = 2\frac{U_\infty}{R}$$

$$u_3 = -\frac{2}{3!}\frac{U_\infty}{R^3}$$

$$u_5 = \frac{2}{5!}\frac{U_\infty}{R^5}$$

$$u_7 = -\frac{2}{7!}\frac{U_\infty}{R^7}$$

$$u_9 = \frac{2}{9!}\frac{U_\infty}{R^9}$$

$$u_{11} = -\frac{2}{11!}\frac{U_\infty}{R^{11}} \qquad \text{(IV-11)}$$

and

$$\eta = \frac{y}{R}\left(\frac{2U_\infty R}{\nu}\right)^{\frac{1}{2}} \qquad \text{(IV-12)}$$

Introduction of the coefficients u_1, u_3, ... into the velociy distribution, Equation IV-5, gives

$$u = 2U_\infty\left[\frac{x}{R} f_1' - \frac{4}{3!}\left(\frac{x}{R}\right)^3 f_3' + \frac{6}{5!}\left(\frac{x}{R}\right)^5 f_5' \ldots\right] \qquad \text{(IV-13)}$$

The velocity of slip is given

$$u_s = \frac{2-\sigma}{\sigma}\lambda\left(\frac{\partial u}{\partial y}\right)_{y = \varkappa} \qquad \text{(IV-14)}$$

where once again λ is the mean free path, and σ is the reflection coefficient. Notice that the gradient is evaluated at the separation distance, $\varkappa$, instead of at the wall. In terms of the dimensionless parameter η, the slip velocity is given as

$$u_s = \frac{2-\sigma}{\sigma}\frac{\lambda}{R}\left(\frac{2U_\infty R}{\nu}\right)^{\frac{1}{2}}\left(\frac{\partial u}{\partial \eta}\right)_{\eta = \eta^*} \qquad \text{(IV-15)}$$

where η^* is given by Equation IV-12 but with y replaced by $\varkappa$. The parameter η^* is a dimensionless form of the separation distance. Also from Equation II-2

$$\frac{\lambda}{R}\left(\frac{2U_\infty R}{\nu}\right)^{\frac{1}{2}} = 1.775\ M\left(\frac{\gamma}{Re}\right)^{\frac{1}{2}} \qquad \text{(IV-16)}$$

where the Reynold number, Re, is equal to $\rho U_\infty R/\mu$. Therefore

$$u_s = 1.775 \frac{2-\sigma}{\sigma} M \left(\frac{\gamma}{Re}\right)^{\frac{1}{2}} \left(\frac{\partial u}{\partial \eta}\right)_{\eta = \eta^*} \qquad \text{(IV-17)}$$

Differentiating Equation IV-13 and substituting into Equation IV-17 leads to

$$u_s(\eta^*) = 3.55 \frac{2-\sigma}{\sigma} M \left(\frac{\gamma}{Re}\right)^{\frac{1}{2}} U_\infty \left\{\frac{x}{R} f_1''(\eta^*) - \frac{4}{3!}\left(\frac{x}{R}\right)^3 f_3''(\eta^*) + \ldots\right\} \qquad \text{(IV-18)}$$

Equating this expression to Equation IV-13 evaluated at η^*, gives the following relation

$$\left(\frac{x}{R}\right) f_1'(\eta^*) - \frac{4}{3!}\left(\frac{x}{R}\right)^3 f'(\eta^*) + \frac{6}{5!}\left(\frac{x}{R}\right)^5 f'(\eta^*) - \ldots =$$

$$1.772 \left(\frac{2-\sigma}{\sigma}\right)\left(\frac{\gamma}{Re}\right)^{\frac{1}{2}} M\left\{\left(\frac{x}{R}\right) f_1''(\eta^*) - \right. \qquad \text{(IV-19)}$$

$$\left. \frac{4}{3!}\left(\frac{x}{R}\right)^3 f_3''(\eta^*) + \frac{6}{5!}\left(\frac{x}{R}\right)^5 f_5''(\eta^*) - \ldots\right\}$$

From Equation IV-19 η^* may be evaluated. By equating like powers of x/R in Equation IV-19 one obtains equations of the form

$$f_k'(\eta^*) = 1.772 \left(\frac{2-\sigma}{\sigma}\right)\left(\frac{\gamma}{Re}\right)^{\frac{1}{2}} M f_k''(\eta^*) \qquad \text{(IV-20)}$$

where k = 1,3,5, ... Thus one can evaluate η^* as a function of $M/(Re)^{\frac{1}{2}}$. All k equations should be identically zero for the same η^*; however, if η^* is determined from the k = 1 equation, and this η^* is substituted into the remaining equations it can be seen that they will not be identically zero(58).

This anomaly implies that η^* is a function of x, which means that the fictitious continuum surface is not circular; however, for the first 180^0 the distortion from a circular surface is less than one percent of the radius. Therefore for the remainder of this analysis the continuum surface will be considered circular, and η^* will be evaluated from

$$f_1'(\eta^*) = 1.772 \left(\frac{2-\sigma}{\sigma}\right)\left(\frac{\gamma}{Re}\right)^{\frac{1}{2}} M f_1''(\eta^*) \qquad \text{(IV-21)}$$

The shearing stress at η^* is given by

$$\tau_x = \mu \left(\frac{\partial u}{\partial y}\right)_x \qquad \text{(IV-22)}$$

or upon substitution from Equations IV-12 and IV-13

$$\tau_{\eta^*} = \frac{2\mu U_\infty}{R}\left(\frac{2U_\infty R}{\nu}\right)^{\frac{1}{2}}\left\{\frac{x}{R} f_1''(\eta^*) - \frac{4}{3!}\left(\frac{x}{R}\right)^3 f_3''(\eta^*) + \cdots\right\} \qquad \text{(IV-23)}$$

The position of the point of separation for a given η^* can be determined from the condition that the shearing stress must vanish at that point (Figure IV-2). This leads to the equation

$$f_1''(\eta^*) - \frac{4}{3!} f_3''(\eta^*)\left(\frac{x}{R}\right)^2 + \frac{6}{5!} f_5''(\eta^*)\left(\frac{x}{R}\right)^4 + \cdots = 0 \qquad \text{(IV-24)}$$

Equation IV-24 may be written in terms of f_k' by substituting from Equation IV-20.

Knowing the point of separation the viscous drag per unit length on the cylinder may be calculated by evaluating

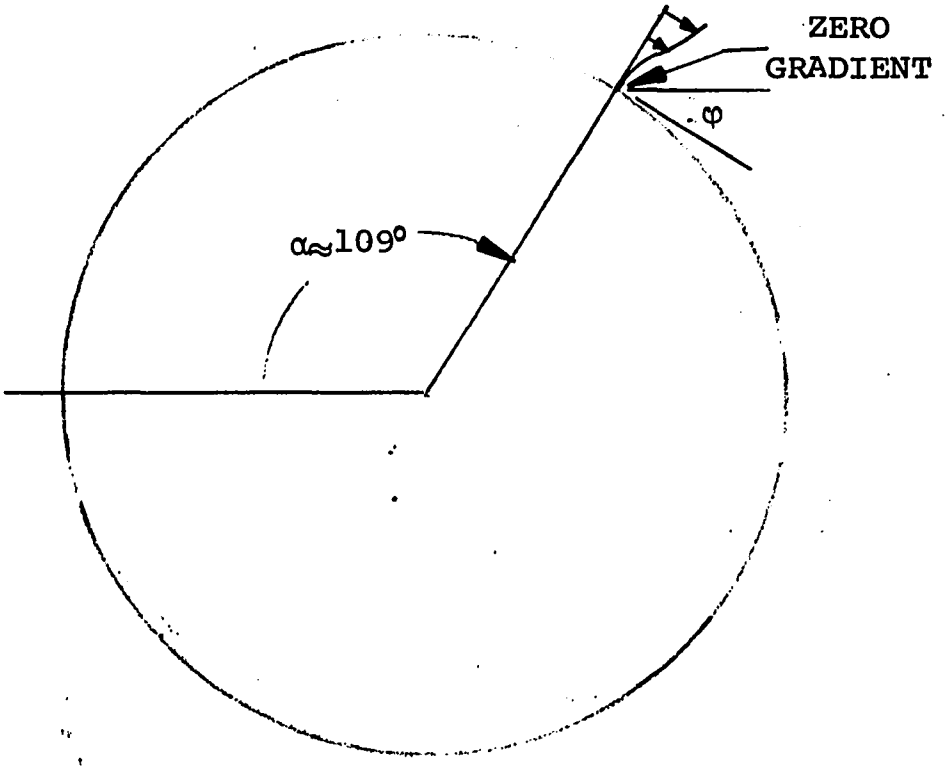

NO SLIP CONDITION

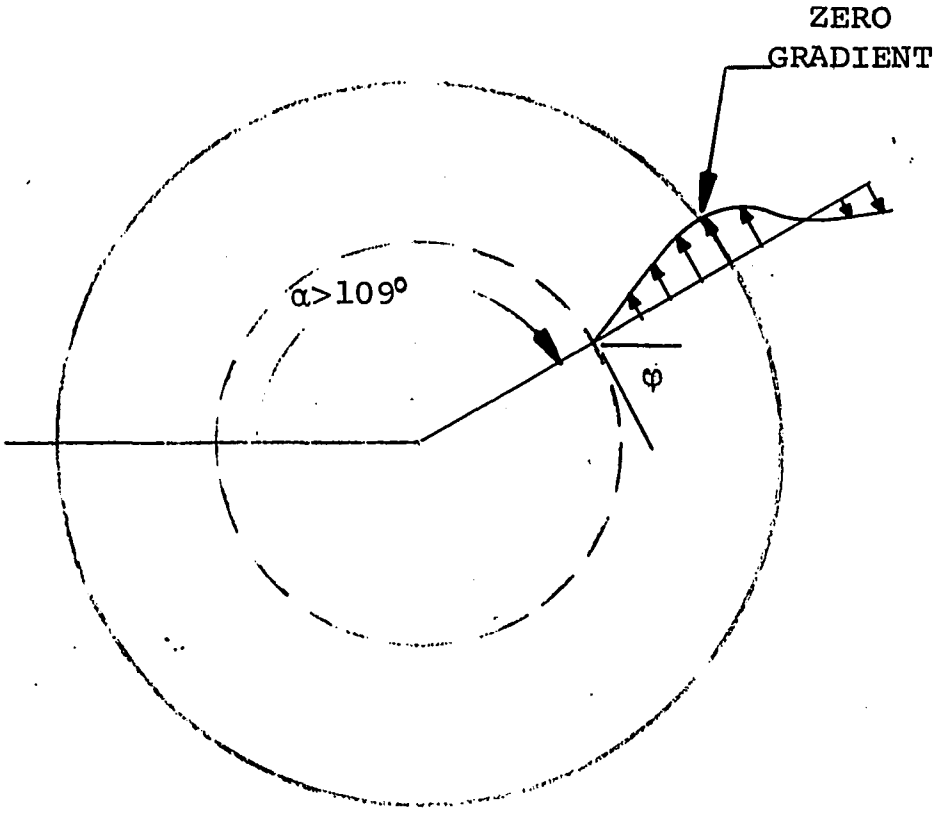

SLIPPING CONDITION

FIGURE IV-2 CYLINDER CROSS SECTION SHOWING ANGLE AT WHICH SEPARATION OCCURS

the integral

$$D_F = \int_0^{\beta(\eta^*)} \tau_{\eta^*} \cos \varphi_a dx_a \qquad \text{(IV-25)}$$

where $\beta(\eta^*)$ is the point of separation given by Equation IV-24; φ_a is the angle between the tangent to the actual surface and the free stream velocity U_∞. Substitution of Equation IV-24 into IV-25 gives

$$D_F = \frac{2\mu U_\infty}{R}\left(\frac{2U_\infty R}{\nu}\right)^{\frac{1}{2}} \int_0^{\beta}\left\{f_1''(\eta^*)\left(\frac{x}{R}\right) - \frac{4}{3!} f_3''(\eta^*)\left(\frac{x}{R}\right)^3 + \ldots\right\} \cos \varphi_a dx_a \qquad \text{(IV-26)}$$

The integral may be evaluated by noting that $\cos \varphi_a = \sin \alpha_a$, and $\alpha_a = \alpha = x/R$. Replacing x with $R\alpha$ and eliminating f_k'' by use of Equation IV-20 leads to

$$D_F = \frac{1.6\ \sigma U_\infty^2 \rho R_a}{(2-\sigma)(\gamma)^{\frac{1}{2}}M} \int_0^{\alpha}\left\{f_1'(\eta^*)\ \alpha - \frac{4}{3!} f_3'(\eta^*)\ \alpha^3 + \ldots\right\} \sin \alpha\, d\alpha \qquad \text{(IV-27)}$$

Integration of Equation IV-27 gives the following for the viscous drag per unit length, D_F on the cylinder

$$D_F = \frac{1.6\ \sigma\rho U_\infty^2 R_a}{(2-\sigma)(\gamma)^{\frac{1}{2}}M}\left\{f_1'(\sin \alpha - \alpha \cos \alpha + 2\sum_{m=1}^{m=5}(m+1) f_{2m+1}'\left[\sum_{n=0}(-1)^n \alpha^{2n}\left(\frac{\sin \alpha}{(2n)!} - \frac{\alpha \cos \alpha}{(2n+1)!}\right)\right]\right\} \qquad \text{(IV-28)}$$

The viscous drag coefficient is defined as

$$C_{D_F} = \frac{D_F}{\rho U_\infty^2 R} \qquad \text{(IV-29)}$$

The details of the integration of Equation IV-27 are given in Appendix C. The integration is carried out from the stagnation point to the point of separation. The results of the integration can be arranged as a sum of easily computed terms, which heretofore has gone unnoticed. The generally accepted formulation for the viscous drag on a right circular cylinder in continuum flow is due to Thom (59, 60). He calculated the viscous drag up to 60° from the forward stagnation point by using a closed form approximate solution of the boundary layer equations, and by taking values between 60° and 90° from experiment, thus deducing $3.84(Re)^{-\frac{1}{2}}$ as the viscous drag coefficient for the front half of the cylinder. With a small addition for the contribution of the rear half, Thom gave $4.0(Re)^{-\frac{1}{2}}$ as a close estimate of this coefficient. The analysis given in Appendix C with η^* equal to zero (i.e., for a continuum) leads to $6.0(Re)^{-\frac{1}{2}}$ for the coefficient. Substituting Equation IV-28 into IV-29 gives

$$C_{D_F} = \frac{1.6\ \sigma\ R_a}{(2-\sigma)\,(\gamma)^{\frac{1}{2}} M\ R} \left\{ f_1' (\sin\alpha - \alpha\cos\alpha) + 2\sum_{m=1}^{m=5} (m+1) f_{2m+1}' \left[\sum_{n=0}^{n=m} (-1)^n\, \alpha^{2n} \left(\frac{\sin\alpha}{(2n)!} - \frac{\alpha\cos\alpha}{(2n+1)!} \right) \right] \right\} \qquad \text{(IV-30)}$$

The total drag for a cylinder is equal to the viscous drag plus the profile, or form, drag; therefore the profile drag must also be taken into account. The profile drag is a function of the pressure differential existing between the front and back of the cylinder and hence the technique of separated cylinders is not necessary in order to estimate the profile drag. Liu and Passamaneck (56) have suggested the following relation for the coefficient of profile drag:

$$C_{D_P} = \frac{2.11}{M + 0.785\ Re_a} \qquad \text{(IV-31)}$$

where Re_a is the Reynolds number based on the radius, R_a, of the actual cylinder. The relation between this Reynolds number and the one previously used can be easily derived by noting that $R_a = R + \varkappa$ (Figure IV-1);

$$Re_a = Re + .707\ \eta^*(Re)^{\frac{1}{2}} \qquad \text{(IV-32)}$$

The total drag coefficient is equal to the sum of Equations IV-30 and IV-31 and is depicted in Figures IV-3 and IV-4 along with the data of Coudeville, et al (61) for Mach numbers of 0.1271 and 0.0322.

B. Flow Past a Wedge

The governing equations for flow past a wedge are the same as those for the circular cylinder, namely, the

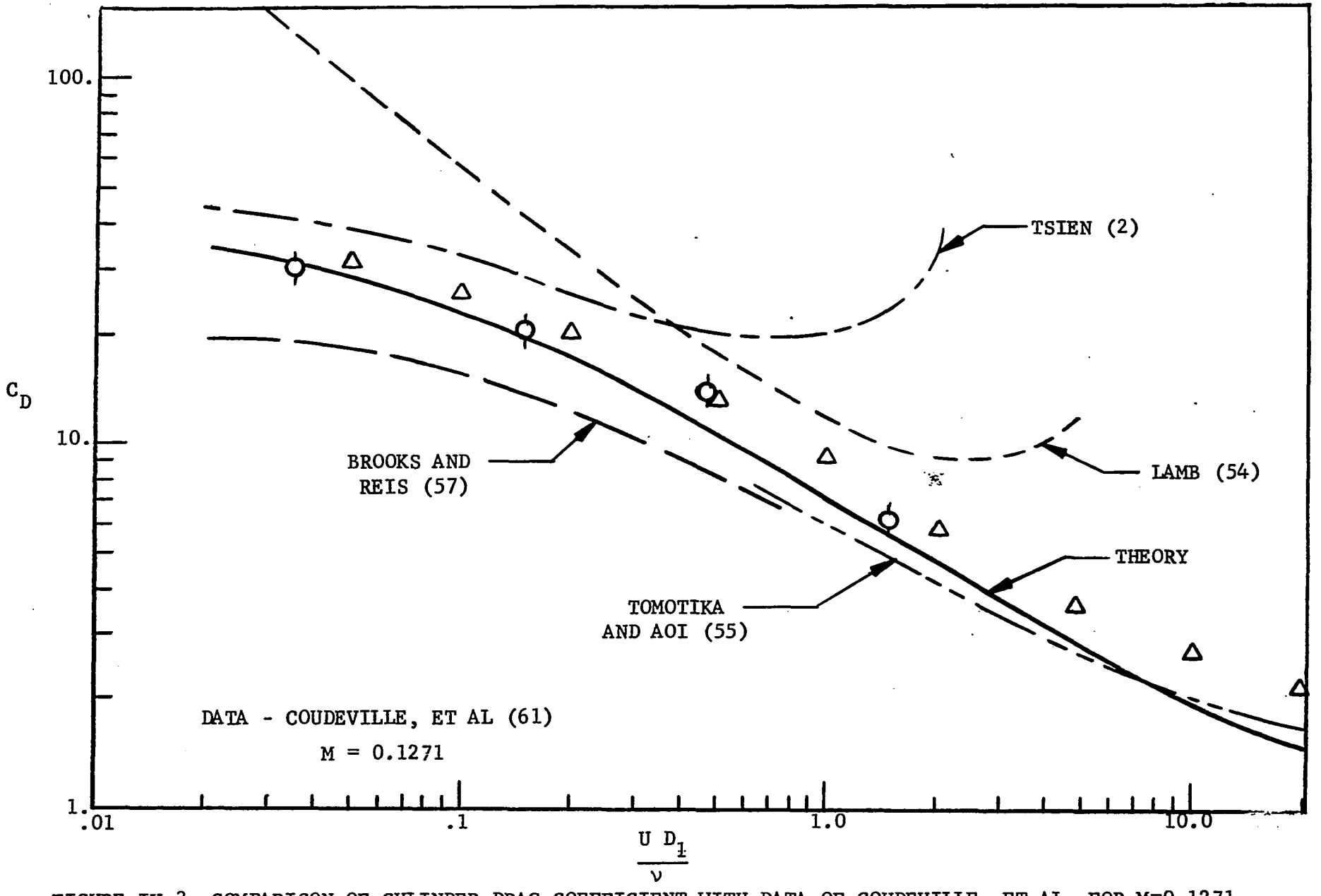

FIGURE IV-3 COMPARISON OF CYLINDER DRAG COEFFICIENT WITH DATA OF COUDEVILLE, ET AL, FOR M=0.1271

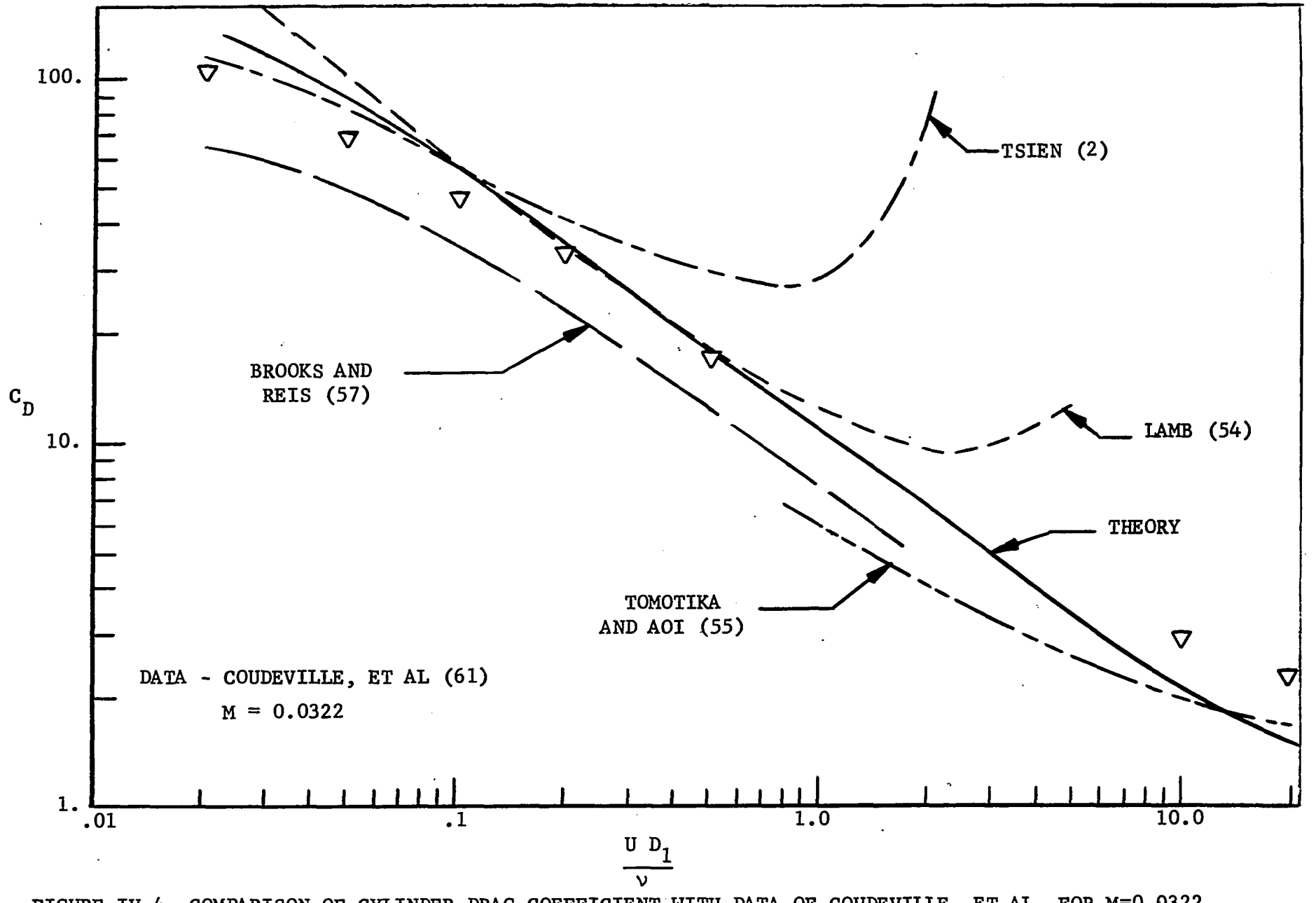

FIGURE IV-4 COMPARISON OF CYLINDER DRAG COEFFICIENT WITH DATA OF COUDEVILLE, ET AL, FOR M=0.0322

continuity equation (Equation IV-1) and the simplified Navier-Stokes equations (Equation IV-2). The stream function, ψ, defined as follows

$$u = \frac{\partial \psi}{\partial y} , \quad v = - \frac{\partial \psi}{\partial x} \tag{IV-32}$$

will satisfy the continuity equation identically. When the stream function is introduced into the Navier-Stokes equation (Equation IV-2), the equation becomes

$$\frac{\partial \psi}{\partial y} \frac{\partial^2 \psi}{\partial x \partial y} - \frac{\partial \psi}{\partial x} \frac{\partial^2 \psi}{\partial y^2} = U \frac{dU}{dx} + \nu \frac{\partial^3 \psi}{\partial y^3} \tag{IV-33}$$

Equation IV-33 may be made dimensionless by substituting the following quantities

$$\xi = \frac{x}{L} , \quad \eta = \frac{[Re]y}{L\, G(x/L)} , \quad f(\xi,\eta) = \frac{[Re]\psi}{LUG(x/L)} \tag{IV-34}$$

where $G(x/L)$ is a scale factor and $Re = U_\infty L/\nu$. Substitution of Equation IV-34 into IV-33 yields

$$f''' + \alpha f f'' + \beta(1-f'^2) = \frac{U}{U_\infty} G^2 \left(f' \frac{\partial f'}{\partial \xi} - f'' \frac{\partial f}{\partial \xi} \right) \tag{IV-35}$$

where the prime, $'$, denotes partial differentiation with respect to η and

$$\alpha = \frac{LG}{U_\infty} \frac{d}{dx}(UG), \quad \beta = \frac{LG^2}{U_\infty} \frac{dU}{dx} \tag{IV-36}$$

The flow past a wedge is one of the few types of local free stream velocity variations leading to similar boundary

layer velocity profiles at all locations, x, along the surface. Mathematically, this simplicity manifests itself by the ready conversion of the governing partial differential equations into total differential equations. Therefore, Equation IV-35 will have similar solutions only when f and f' do not depend on ξ (i.e. when the right hand side of the equation is zero). Simultaneously the coefficients α and β on the left side of the equation must be independent of x (i.e. they must be constant). This latter condition, combined with Equation IV-36, furnishes two equations for determining the local free stream velocity, U, and the scale factor, G. Simultaneous solution of these two equations leads to

$$U = U_\infty K \left(\frac{2}{m+1}\frac{x}{L}\right)^m$$

and

$$G = \left(\frac{2}{m+1}\frac{x}{L}\frac{U_\infty}{U}\right)^{\frac{1}{2}} \qquad \text{(IV-37)}$$

where K is a constant and $m = \beta/(2-\beta)$. It is thus concluded that similar solutions of the boundary layer equations are obtained when the local free stream velocity, U, is proportional to a power of x measured along the surface from the stagnation point. It will now be shown that the potential flow velocity along the surface of a wedge whose included angle is $\pi\beta$ (Figure IV-5) is given as $U = Cx^m$. From potential theory the complex velocity, dW/dz, is related to the

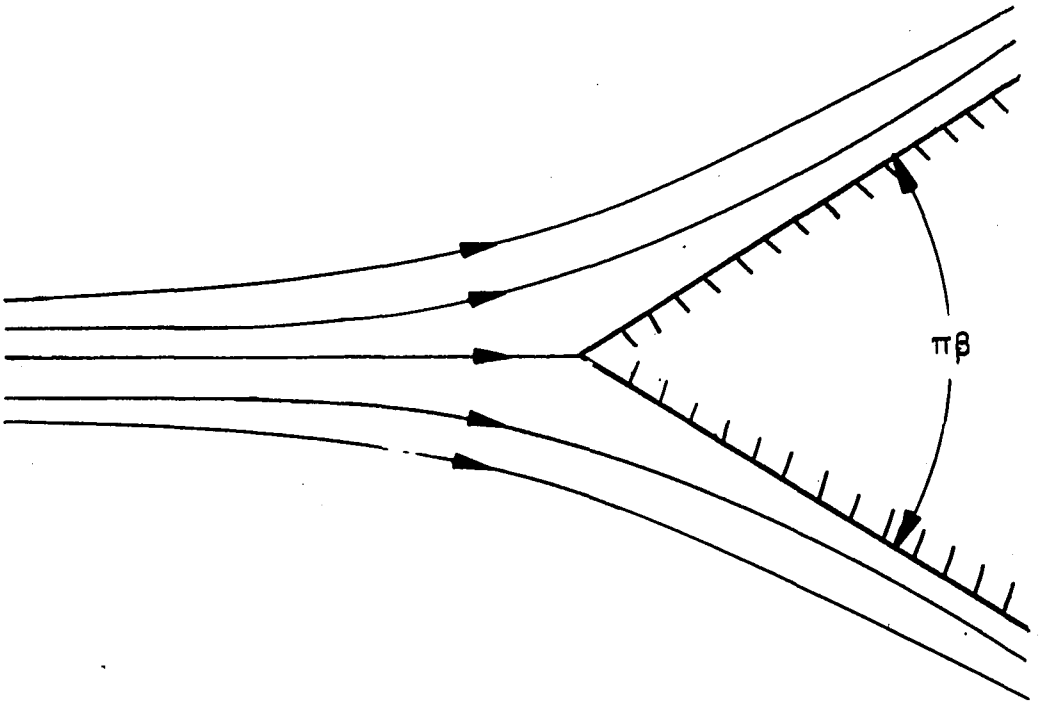

FIGURE IV-5 CROSS SECTION OF WEDGE

local free stream velocity, U, by

$$\frac{dW}{dz} = \frac{\partial \varphi}{\partial x_1} + i \frac{\partial \psi}{\partial x_1} = u_1 - iv_1 = Ue^{-i\alpha} \qquad \text{(IV-38)}$$

where $z = x_1 + iy_1$, φ is the potential function, ψ is the stream function, U is the local free stream velocity and α is its inclination as shown in Figure IV-6. For flow about a wedge W is assumed to be (62)

$$W = Az^{\frac{\pi}{\alpha}} \qquad \text{(IV-39)}$$

thus

$$\frac{dW}{dz} = \frac{\pi}{\alpha} Az^{\frac{\pi}{\alpha} - 1} \qquad \text{(IV-40)}$$

$$= \frac{\pi}{\alpha} Ar^{\frac{\pi}{\alpha} - 1} \left[\cos\left(\frac{\pi}{\alpha} - 1\right)\gamma + i \sin\left(\frac{\pi}{\alpha} - 1\right)\gamma\right]$$

Therefore

$$u_1 = \frac{\pi}{\alpha} Ar^{\frac{\pi}{\alpha} - 1} \cos\left(\frac{\pi}{\alpha} - 1\right)\gamma \qquad \text{(IV-41)}$$

and

$$v_1 = -\frac{\pi}{\alpha} Ar^{\frac{\pi}{\alpha} - 1} \sin\left(\frac{\pi}{\alpha} - 1\right)\gamma \qquad \text{(IV-42)}$$

or at $\gamma = \alpha$

$$u_1 = \frac{\pi}{\alpha} Ar^{\frac{\pi}{\alpha} - 1} \cos(\pi - \alpha) \qquad \text{(IV-43)}$$

and

$$v_1 = -\frac{\pi}{\alpha} Ar^{\frac{\pi}{\alpha} - 1} \sin(\pi - \alpha) \qquad \text{(IV-44)}$$

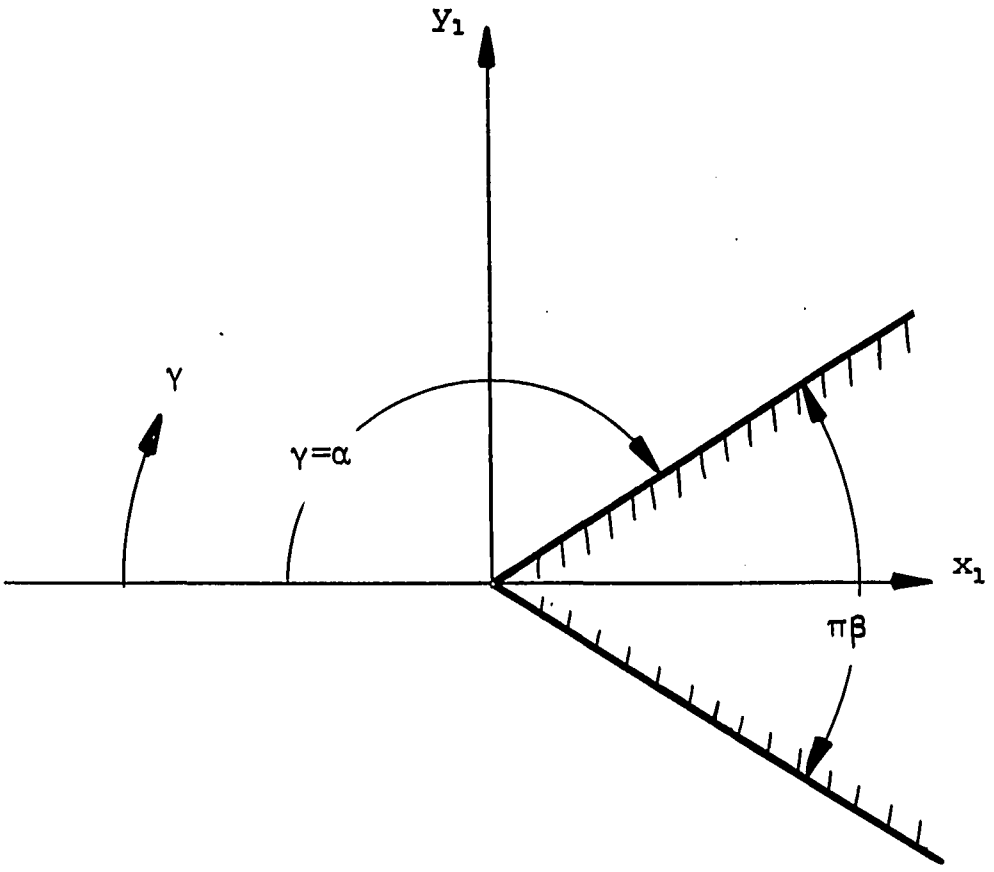

FIGURE IV-6 WEDGE CROSS SECTION SHOWING POTENTIAL FLOW COORDINATE REFERENCES AND ANGLES

Hence

$$U = (\ddot{u}_1^2 + v_1^2)^{\frac{1}{2}} = \frac{\pi}{\alpha} Ar^{\frac{\pi}{\alpha} - 1} \qquad \text{(IV-45)}$$

but $\alpha = \pi(1 - .5\beta)$; therefore Equation IV-45 reduces to

$$U = \frac{\pi}{\alpha} Ar^{\frac{\beta}{2-\beta}} \qquad \text{(IV-46)}$$

Or since $m = \beta/(2-\beta)$

$$U = \frac{\pi}{\alpha} Ar^m \qquad \text{(IV-47)}$$

$$= Cr^m$$

If x is measured along the surface, then the r in Equation IV-47 is the same as x; therefore

$$U = Cx^m \qquad \text{(IV-48)}$$

And thus it is shown that the flow about a wedge is of the form that will lead to "similar" solutions of the boundary layer equations.

Equation IV-35 with the right side equal to zero was first given by Falkner and Skan (63). Hartree (64) carefully integrated this equation and obtained velocity profiles for various values of β (Figure IV-7). The relation between u and f is

$$u = \frac{\partial \psi}{\partial y} = U \frac{\partial f}{\partial \eta} = Uf' \qquad \text{(IV-49)}$$

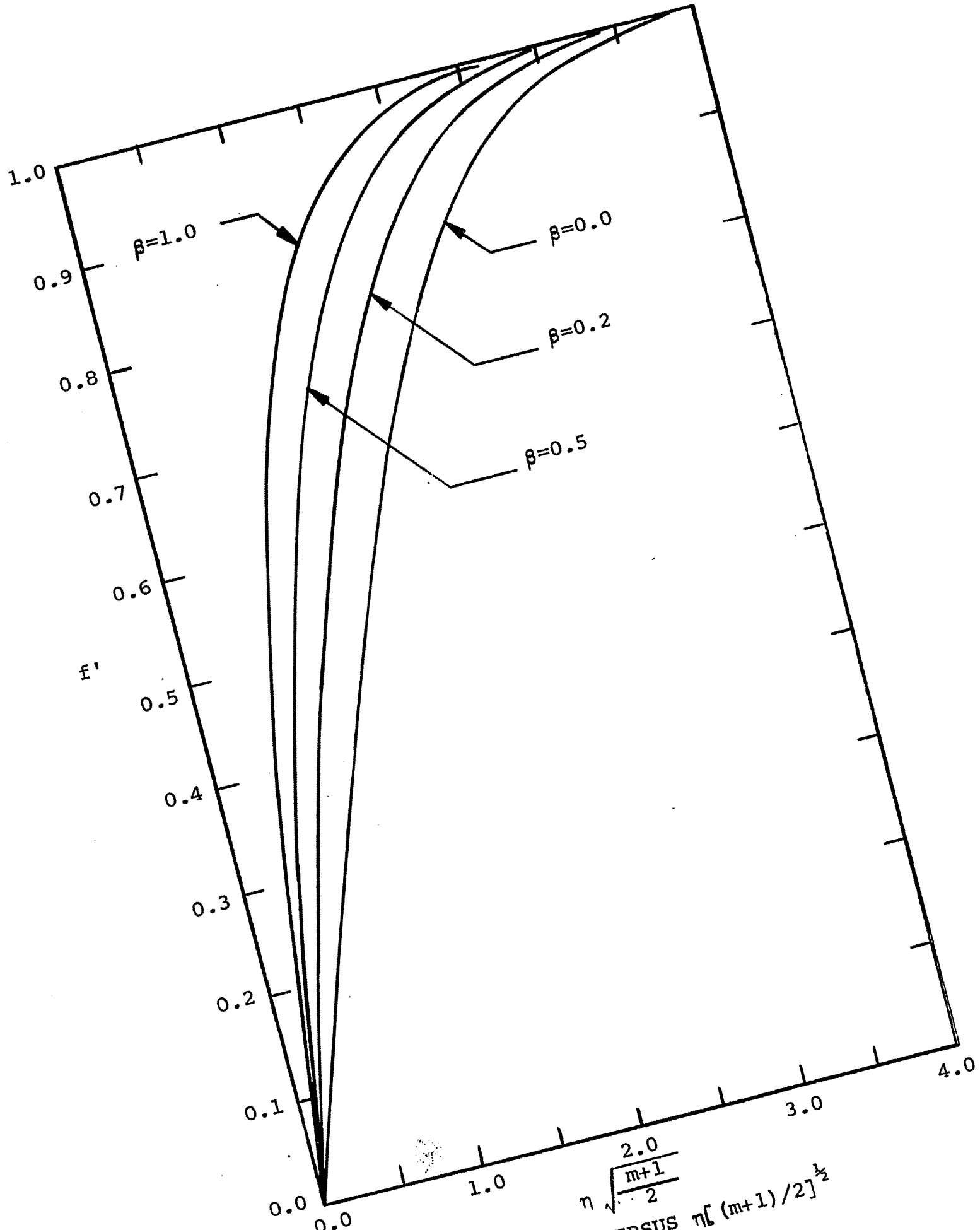

FIGURE IV-7 f' VERSUS $\eta[(m+1)/2]^{\frac{1}{2}}$

Once again the separation distance, $\varkappa$, between the superimposed wedges (Figure IV-8), may be obtained by matching the slip velocity to the velocity evaluated at $\varkappa$.

$$u_s = \lambda \left(\frac{\partial u}{\partial y}\right)_{y = \varkappa} = \lambda \left(\frac{\partial \eta}{\partial y} \frac{\partial u}{\partial \eta}\right)_{\eta = \eta^*} \tag{IV-50}$$

where η^* is η evaluated at $y = \varkappa$, and σ has been assumed to be equal to unity for simplicity. The expression for η is given by Equation IV-34 with G given by Equation IV-37. Substituting into Equation IV-50 yields

$$u_s = \lambda \left(\frac{m+1}{2} \frac{U}{\nu x}\right)^{\frac{1}{2}} \left(\frac{\partial u}{\partial \eta}\right)_{\eta = \eta^*} \tag{IV-51}$$

Equation IV-49 may be substituted for u in Equation IV-51 to give

$$u_s = \frac{\lambda}{x} \left(\frac{m+1}{2} \mathrm{Re}\right)^{\frac{1}{2}} U f''(\eta^*) \tag{IV-52}$$

where $\mathrm{Re}=Ux/\nu$. The tangential velocity, Equation IV-49, becomes

$$u_s = U f'(\eta^*) \tag{IV-53}$$

Therefore, equating Equations IV-52 and IV-53 and substituting Equation I-3 for the mean free path, λ, yields

$$f'(\eta^*) = 1.26 \left(\frac{m+1}{2} \frac{\gamma}{\mathrm{Re}}\right)^{\frac{1}{2}} M f''(\eta^*)$$

or

$$\frac{f'(\eta^*)}{f''(\eta^*)} = 1.26 \left(\frac{m+1}{2} \frac{\gamma}{\mathrm{Re}}\right)^{\frac{1}{2}} M \tag{IV-54}$$

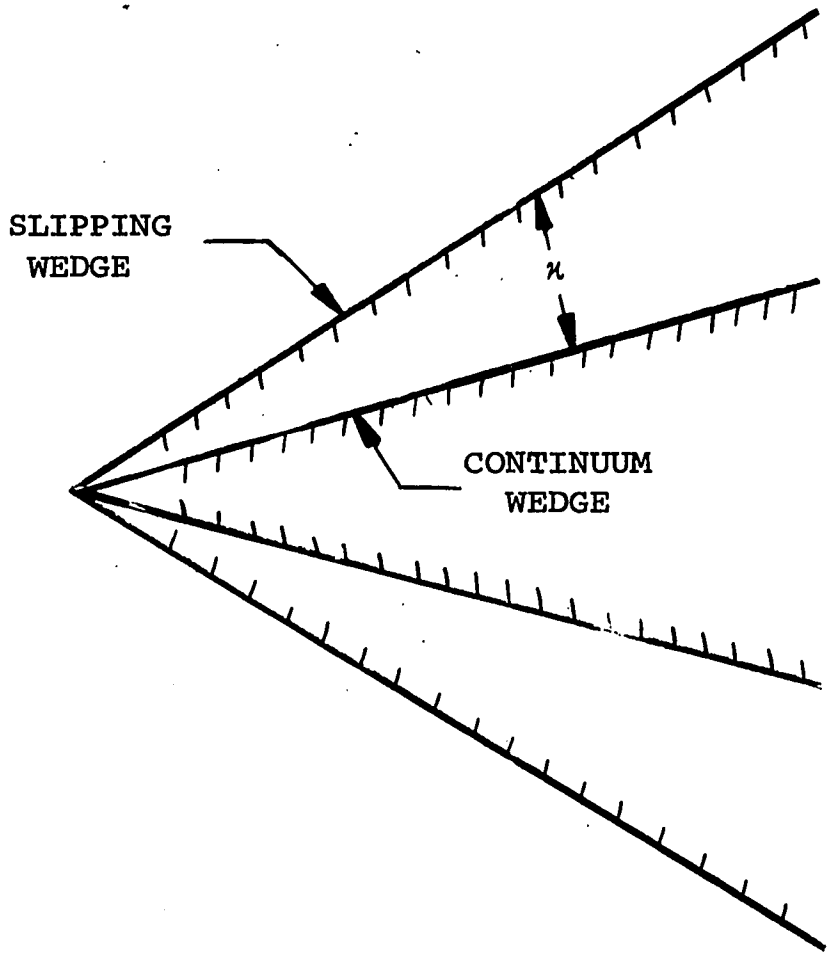

FIGURE IV-8 SUPERPOSITON OF SLIPPING AND NONSLIPPING WEDGES

where f' is plotted in Figure IV-7. $f''(\eta^*)$ is obtained graphically from the data of f' as given in reference 64.

The parameter η^* may be evaluated by use of Equation IV-54 and Figure IV-9. For a value of $1.26\ M(\gamma/Re)^{\frac{1}{2}}$, which is a measure of the degree of slip, one can calculate the corresponding value of f'/f'' from Equation IV-54. With this value one can read off from the appropriate curve of Figure IV-9 the value of η^*.

The shear stress is given as

$$\tau = \mu \left(\frac{\partial u}{\partial y}\right)_{y = \varkappa} = \mu \left(\frac{m+1}{2} \frac{U}{\nu x}\right)^{\frac{1}{2}} \left(\frac{\partial u}{\partial \eta}\right)_{\eta = \eta^*} \qquad \text{(IV-55)}$$

Substituting for u from Equation IV-49 and differentiating yields

$$\tau_{\eta^*} = \mu \left(\frac{m+1}{2} \frac{U}{\nu x}\right)^{\frac{1}{2}} U f''(\eta^*) \qquad \text{(IV-56)}$$

The skin friction coefficient, c_F, for a wedge is given as (65)

$$c_F = \frac{\tau_{\eta^*}}{\rho U^2} (Re)^{\frac{1}{2}} \qquad \text{(IV-57)}$$

The shear stress, τ_{η^*}, may be eliminated by use of Equation IV-56, also f'' may be replaced by its equivalent expression, Equation IV-54, thus Equation IV-57 becomes

$$c_F = .795 \frac{1}{M} \left(\frac{Re}{\gamma}\right)^{\frac{1}{2}} f'(\eta^*) \qquad \text{(IV-58)}$$

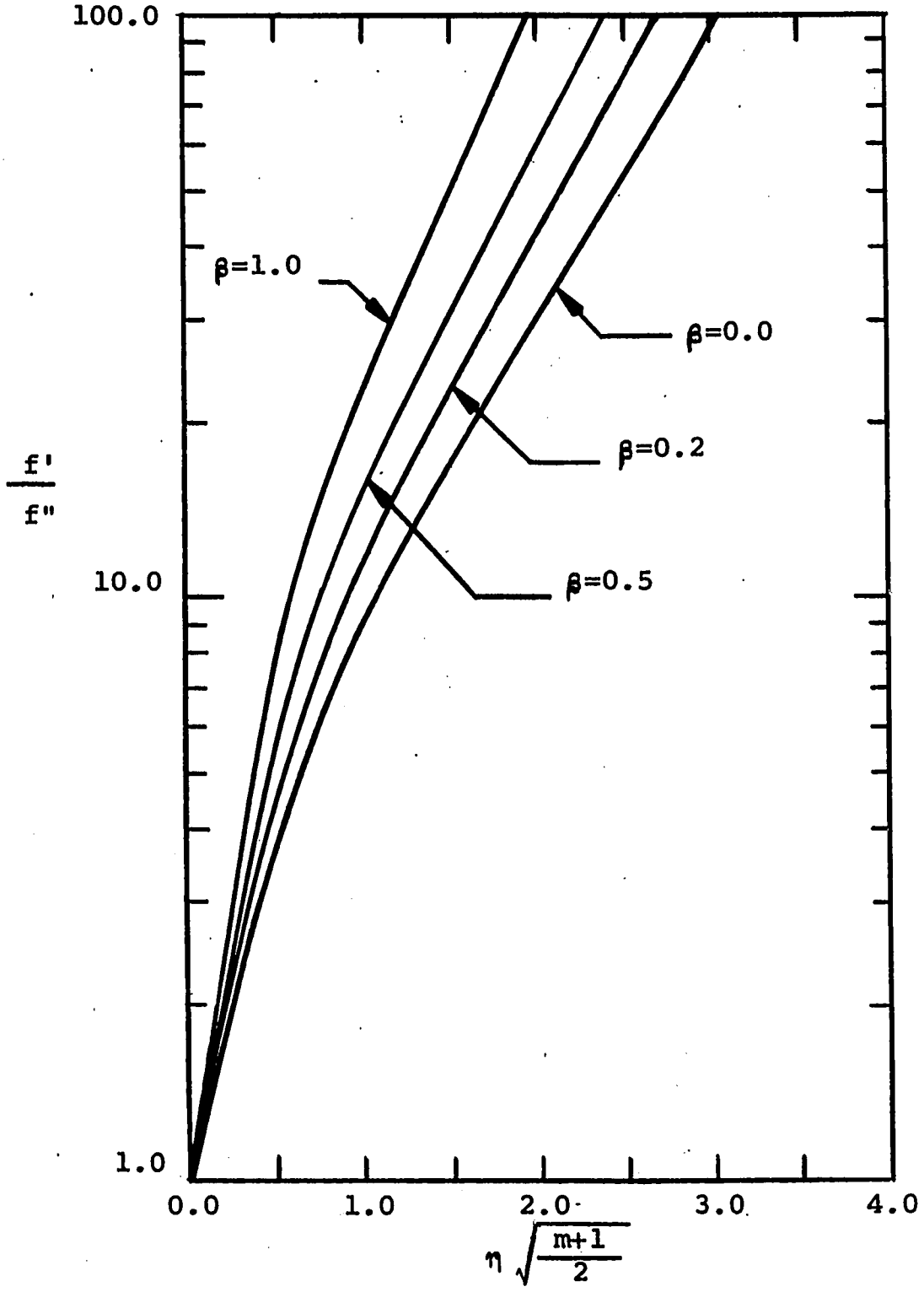

FIGURE IV-9 f'/f" VERSUS $\eta[(m+1)/2]^{\frac{1}{2}}$

CHAPTER V

CONCLUSION

A new method of analyzing rarefied slip flow problems has been developed. The method was applied to the problems of Rayleigh, Couette and Poiseuille flow, and to flow through rectangular and triangular cross section ducts and flow past a cylinder and a wedge.

The Navier-Stokes equations were used as the governing equations since these are considered (5) to be superior to kinetic theory equations for this type of flow.

In all cases the expressions for the various flow parameters agree in the limit with those predicted by continuum theory.

Also a new expression for the skin-friction drag coefficient in continuum flow was derived.

A. Rayleigh's Problem

The Rayleigh problem for flow over a flat plate was analyzed. The Rayleigh problem is not the best analysis of the flow over a flat plate (the Blasius approach to the problem is better); however, the Rayleigh method was chosen, due to its simplicity, only as a means of introducing the aforementioned new technique for solving rarefied flow prob-

lems. Nevertheless, there is still surprisingly good agreement between the theory given here and the experimental data taken by Schaaf and Sherman (66) at the Berkeley Low-Pressure wind tunnel (Figure II-3).

A fruitful area for further study could be the application of this technique to a flat plate using Blasius' approach.

An interesting point of this analysis is that the average drag coefficient, Equation II-39, predicts a peak value that is exactly equal to the experimentally verified free molecule value; whereas, the value given by Mirels, Equation II-32, gives a somewhat higher value (Figure II-2).

B. Couette Flow

The analysis given for Couette flow predicts values for the skin-friction, Equation III-10, which agree with continuum theory when there is no slip and also agree with the free molecule values for large degrees of slip. The equation has excellent agreement with the experimental data of F.S. Chiang (67) from one flow extreme to the other (Figure III-2).

C. Poiseuille Flow

A pressure drop correction coefficient, φ, was derived for Poiseuille flow. For a given pressure drop, the resulting flow is φ times the value predicted by continuum theory with no slip. Flow rates up to 40,000 times greater than predicted

by the Hagen-Poiseuille law have been reported for free molecule flow. Equation III-28 predicts correction coefficient values (Figure III-4) which are in very good agreement with the data of Brown, et al (68).

D. Flow Past A Cylinder

An expression has been developed for the coefficient of drag for a right circular cylinder. This expression predicts values which are in agreement with the data of Coudeville, et al (61) as can be seen in Figures IV-3 and IV-4. It also appears to fit the data over a larger range of Reynolds numbers than does any of the other existing theories. It should also be noted that the theory given here is based on the Blasius exact solution of the Navier-Stokes equations and not upon approximations (i.e. perturbations) as are the other theories.

During the analysis of the rarefied flow past a cylinder a new continuum result for the skin-friction drag coefficient was obtained. The value predicted was $6(Re)^{-\frac{1}{2}}$; whereas the generally accepted value is given as $4(Re)^{-\frac{1}{2}}$ (Figure C-2). Again, the value of $4(Re)^{-\frac{1}{2}}$ is based on an integration by Thom of his closed form approximate boundary layer equation for the front 60° of the cylinder and then from 60° to 90° he used experimental data. For the back half of the cylinder Thom guessed at a value. He combined the results for the

three areas and gave $4(Re)^{-\frac{1}{2}}$ as an approximate value for the overall cylinder.

E. Rectangular and Triangular Duct Flow and Flow Past a Wedge

Equations are given for the pressure drop coefficient, Λ, Equation III-37 and III-47, for flow through a rectangular and triangular duct, respectively. Also an expression was derived for the skin-friction on a wedge, Equation IV-58. The author could find no applicable experimental data for the above types of flows; however, the equations given do predict the correct continuum limit in all cases.

REFERENCES

1. Maxwell, J. C., The Scientific Papers of James Clerk Maxwell, Vol. 2, Cambridge University Press, 1890.

2. Tsien, H. S., "Superaerodynamics, Mechanics of Rarefied Gases," Journal of the Aeronautical Sciences, 13, pp 653-664 December, 1946.

3. Tsien, H. S., Wind Tunnel Testing Problems in Superaerodynamics, Journal of the Aeronautical Sciences, 15, pp 573-580 October, 1948.

4. Chapman, S., "On the Law of Distribution of Molecular Velocities, and on the Theory of Viscosity and Thermal Conduction, in a Non-Uniform Simple Monatomic Gas," Phil. Trans. Roy. Soc., Vol. 216(A), 1915.

5. Schaaf, S. A., and Chambre, P. L., "Flow of Rarefied Gases," Section H, Fundamentals of Gas Dynamics, Emmons H. W., ed., Princeton University Press, 1st Ed.,1958.

6. Schaaf, S. A., Chapters 9 and 10, Heat Transfer Symposium-University of Michigan, 1953.

7. Schaaf, S. A., "Recent Progress in Rarefied Gas Dynamics Research," Proceedings of the Sixth Midwestern Conference on Fluid Mechanics, University of Texas, 1959.

8. Nestler, D. N., "Survey of Theoretical and Experimental Determination of Skin Friction in Compressible Boundary Layers." Part V - The Effects of Slip Flow, United States Department of Commerce, AD607831, 1959.

9. Burnett, D., "The Distribution of Molecular Velocities and the Mean Motion in a Nonuniform Gas," Proceedings of London Mathematical Society, Vol. 40, 1935.

10. Grad, H., "On the Kinetic Theory of Rarefied Gases," Communications of Pure and Applied Mathematics, Vol. 2, 1949.

11. Street, R. E., "Problem of Slip Flow in Aerodynamics," NACA RM 57A30, 1957.

12. Wang-Chang, C. S., and Uhlenbeck, G. E.,"Transport Phenomena in Polyatomic Gases," University of Michigan Engineering Research Institute Report, CM681, 1951.

13. Ikenberry, E., and Truesdell, C., "On the Pressures and the Flux of Energy in a Gas According to Maxwell's Kinetic Theory," Parts I and II, Journal of Rational Mechanics and Analysis, Vol. 5, No. 1, 1956.

14. Knudsen, M., "Die Molekulare Warmeleitung der Gase und der Alkommodationskoefficient," Annalen der Physik, Vol. 34, pp 593-656, 1911.

15. Millikan, R. A., "Coefficients of Slip in Gases and the Law of Reflection from Surfaces of Solids and Liquids," Physical Review, Vol. 21, pp 217-238, 1923.

16. Yang, H. T., and Lees, L., "Rayleigh's Problem at Low Mach Number According to Kinetic Theory Approach," Journal of Mathematics and Physics, Vol. 35, No. 3, October 1956.

17. Yang, H. T., and Lees, L., "Rayleigh's Problem at Low Reynolds Number According to the Kinetic Theory of Gases," Rarefied Gas Dynamics, edited by F. M. Devienne, Pergamon Press, New York, 1960.

18. Lees, L., "A Kinetic Theory Description of Rarefied Gas Flows," GALCIT Hypersonic Research Project, Memo. n. 51, December 1959.

19. Gross, E. P., and Jackson, E. A., "Kinetic Theory of the Impulsive Motion of an Infinite Plane," Physics of Fluids, Vol. 1, No. 4, July-August 1958.

20. Gross, E. P., and Jackson, E. A., "Kinetic Models and Linearized Boltzmann Equation," Physics of Fluids, Vol. 2, No. 4, July-August 1959.

21. Broadwell, J. E., "Study of Rarefied Shear Flow by Discrete Velocity Method," Journal of Fluid Mechanics, Vol. 19. pt. 3, July 1964.

22. Cercignani C., and Sernagiotto, F., "Method of Elementary Solutions for Time Dependent Problems in Linearized Kinetic Theory," Annals of Physics, Vol. 30, No. 1, October 1964.

23. Cercignani, C., and Sernagiotto, F., "Rayleigh Problem at Low Mach Numbers According to Kinetic Theory," Rarefied Gas Dynamics, Supplement 3, Vol. 1, Academic Press, New York, 1965.

24. Mirels, H., "Estimate of Slip Effect on Compressible Laminar-Boundary-Layer Skin Friction," NACA TN 2609, 1952.

25. Schaaf, S. A., "A Note on the Flat Plate Drag Coefficient," University of California ER-HE-150-66, 1950.

26. Russo, E. P., and Arnas, O. A., "On a New Approach to Slip Flow Using Rayleigh's Problem," Paper No. 67-WA/APM-18, Journal of Applied Mechanics, to be published.

27. Illingworth, C. R., "Unsteady Laminar Flow of Gas Near an Infinite Flat Plate," Proceedings of Cambridge Philosophical Society, Vol. 46, pt. 4, October 1950.

28. Howarth, L., "Some Aspects of Rayleigh's Problem for a Compressible Fluid," Quarterly Journal of Mechanics and Applied Mathematics, Vol. IV, pt. 2, June 1951.

29. Chapman, D. R., and Rubesin, M. W., "Temperature and Velocity Profiles in the Compressible Laminar Boundary Layer with Arbitrary Distribution of Surface Temperature," Journal of Aeronautical Sciences, Vol. 16, No. 9, September 1949.

30. Crocco, L., "The Laminar Boundary Layer in Gases," Trans. No. F-TS-5053-RE, ATI No. 28323, CADO, Air Material Command Wright Field.

31. Rayleigh, "On the Motion of Solid Bodies Through Viscous Liquid," Phil. Mag. 21, 1911.

32. Hagen, G., "Uber die Bewegung des Wassers in Engen Zylindrischen Rochren," Poggendorff's Annalen d. Physik u. Chemie 2, 1839.

33. Poiseuille, J. L., "Recherches Experimentales sur des Liquides Dans Les Tubes des Tres Petits Diameters," Parts I, II and III, Comptes Rendus. L' Academie des Sciences, 1840-41.

34. Knudsen, M., "Die Gesetz der Molekularstromung und der Innern Reibungsstromung der Gase Durch Robren," Annalen der Physik, Vol. 28, 1908.

35. Gaede, W., "Die Aussere Reibung der Gase," Annalen der Physik, Vol. 4, 1913.

36. Smoluchowski, M. von., "Zur Kinetischen Theorie der Transpuation und Diffusion Verdunnter Gase," Annalen der Physik, Vol. 33, 1910.

37. Pai, S., "Viscous Flow Theory," Volume 1, D. Van Nostrand Company, New Jersey, 1956.

38. Knudsen, M., Kinetic Theory of Gases, Methuen, London, 1950.

39. Cercignani, C., "Plane Poiseuille Flow and Knudsen Minimum Effect," Rarefied Gas Dynamics, Laurmann, J., ed., Supplement 2, 1963.

40. Takao, K., "Rarefied Gas Flow Between Two Parallel Plates," Rarefied Gas Dynamics, Talbot, L., ed., Supplement 1, 1961.

41. De Marcus, W., "The Problem of Knudsen Flow," Union Carbide Nuclear Company, Report K-1302, Oak Ridge, Tennessee, 1957.

42. Milligan, M., "Nozzle Characteristics in the Transition Regime Between Continuum and Free Molecule Flow," AIAA Journal, 1:1088-1092, 1964.

43. Estermann, I., "Gases at Low Densities," Section I, Thermodynamics and Physics of Matter, Rossini, F. D., ed., 1955.

44. Dushman, S., and Lafferty, J. M., Scientific Foundations of Vacuum Technique, 1962.

45. Guthrie, A., and Wakerling, R. K., Vacuum Equipment and Techniques, 1949.

46. Street, R. E., "Plane Couette Flow by the Method of Moments," Rarefied Gas Dynamics, Talbot, L., ed., Supplement 1, 1961.

47. Wang Chang, C. S., and Uhlenbeck, G. E., "The Couette Flow Between Two Parallel Plates as a Function of the Knudsen Number," University of Michigan, Engineering Research Institute Report, 1999-I-T, 1954.

48. Yang, H. T., and Lees, L., "Plane Couette Flow at Low Mach Number According to the Kinetic Theory of Gases," Proceeding of 5th Midwestern Conference on Fluid Mechanics, Ann Arbor, Michigan, 1957.

49. Willis, D. R., "The Effect of the Molecular Model on Solutions to Linearized Couette Flow with Large Knudsen Number," Rarefied Gas Dynamics, Talbot, L., ed., Supplement 1, 1961.

50. Hamel, B., and Wachman, M., "A Discrete Ordinate Technique for the Linearized Boltzmann Equation with Application to Couette Flow," Rarefied Gas Dynamics, de Leeuw, J. H., ed., Supplement 3, 1965.

51. Onufriev, A. T., "Solution of the Linearized Couette Flow Problem in a Rarefied Gas by the Integral Diffusion Method," Journal of Applied Mechanics and Technical Physics, No. 2, translated from Russian, Faraday Press, 1967.

52. Brundin, C. L., ed., Rarefied Gas Dynamics, Section II-3, Supplement 4, Volume 1, 1967.

53. Schlichting, H., Boundary Layer Theory, McGraw-Hill, 1960.

54. Lamb, H., Hydrodynamics, Cambridge University Press, London, 1932.

55. Tomotika, S., and Aoi, T., "The Steady Flow of Viscous Fluid Past a Sphere and Circular Cylinder at Small Reynolds Numbers," Quarterly Journal of Mechanics and Applied Mathematics, 1950.

56. Lin, C. Y., and Passamaneck, R., "Kinetic Theory Description of Flow Over a Cylinder at Low Speeds," Rarefied Gas Dynamics, Brundin, C. L., ed., Supplement 4, Volume I, 1967.

57. Brooks, W. B., and Reis, G. E., "Drag on a Right Circular Cylinder in Rarefied Flow at Low Speed-Ratios," Rarefied Gas Dynamics, Laurmann, J., ed., Supplement 2, Volume II, 1963.

58. Tifford, A. N., "Heat Transfer and Frictional Effects in Laminar Boundary Layers," Part 4, WADC Technical Report, 53-288, 1954.

59. Thom, A., A.R.C. Reports and Memoranda, No. 1194, 1929.

60. Thom, A., Modern Developments in Fluid Dynamics, Goldstein, S., ed., Volume II, p. 425, 1938.

61. Coudeville, H., Trepand, P., and Brun, E., "Drag Measurements in Slip and Transition Flow," Rarefied Gas Dynamics, de Leeuw, J., ed., Supplement 3, Volume 1, 1965.

62. Streeter, V. L., Fluid Dynamics, McGraw-Hill, 1948.

63. Falkner, V. M., and Skan, S. W., "Some Approximate Solutions of the Boundary Layer Equations," British Air Ministry, R. and M. 1314, 1930.

64. Hartree, D. R., "On an Equation Occurring in Falkner and Skan's Approximate Treatment of the Equation of the Boundary Layer," Proceedings of the Cambridge Philosophical Society, 33, Part 2, April 1937.

65. Tifford, A. N., and Chu, S. T., "Heat Transfer and Frictional Effects in Laminar Boundary Layers," Part 1, WADC Technical Report, 53-288, 1953.

66. Schaaf, S. A., and Sherman, F. S., "Skin Friction in Slip Flow," Journal of the Aeronautical Sciences, 21, 1954.

67. Chiang, F. S., "Drag Forces on Rotating Cylinders at Low Pressures," Ph.D. Dissertation, University of California, 1952.

68. Brown, G. P., Di Nardo, A., Cheng, G. K., and Sherwood, T. K., Journal of Applied Physics, 17, 1946.

69. Hildebrand, F.B., Advanced Calculus for Engineers, Prentice-Hall, 1960.

70. Rouse, H., ed., Advanced Mechanics of Fluids, John Wiley, 1959.

71. Russo, E. P., and Arnas, O. A., "A New Solution for the Skin-Friction Drag on a Cylinder," submitted to Physics of Fluids, 1967.

72. Linke, V. W., Physikalische Zeitschrift, p. 908, volume 32, 1931.

APPENDIX A

DERIVATION OF THE VELOCITY PROFILE IN A RECTANGULAR DUCT

DERIVATION OF THE VELOCITY PROFILE IN A RECTANGULAR DUCT

The details of the solution of Equation III-30 for a rectangular duct are given in this Appendix. The Navier-Stokes equation for the flow through a rectangular duct is (Equation III-30)

$$\frac{\partial^2 u}{\partial y^2} + \frac{\partial^2 u}{\partial z^2} = C \qquad \text{(A-1)}$$

where $C = [dp/dx]/(\rho\mu)$. The homogeneous form of Equation A-1 (i.e. the right hand side equal to zero) may be solved by separation of variables by assuming that $u = Y(y)\ Z(z)$. Substitution into Equation A-1 yields

$$ZY'' + YZ'' = 0 \qquad \text{(A-2)}$$

where the primes, ', denotes differentiation with respect to the independent variable. Equation A-2 may be rearranged to give

$$-\frac{Y''}{Y} = \frac{Z''}{Z} = K^2 \qquad \text{(A-3)}$$

where K is a positive constant. Equation A-3 may be separated into the following two ordinary differential equations

$$Y'' + K^2 Y = 0 \qquad \text{(A-4)}$$

and

$$Z'' - K^2 Z = 0 \qquad \text{(A-5)}$$

The solutions of Equations A-4 and A-5 are, respectively,

$$Y = A \sin Ky + B \cos Ky \tag{A-6}$$

and

$$Z = D \sinh Kz + E \cosh Kz \tag{A-7}$$

where A, B, D and E are constants which will be determined from the boundary conditions. The most general particular solution for this problem is

$$u_p = Fy^2 + Gy + H + Rz^2 + Sz \tag{A-8}$$

where F, G, H, R and S are constants. Therefore since $u = YZ + u_p$ the general solution for the velocity u is

$$u = (A \sin Ky + B \cos Ky)(D \sinh Kz + E \cosh Kz) + Fy^2 + Gy + H + Rz^2 + Sz \tag{A-9}$$

The boundary conditions are

$$u = 0 \text{ at } y = 0,\ y = a,\ z = 0,\ z = b \tag{A-10}$$

Substituting $u = 0$ at $y = 0$ yields

$$0 = B(D \sinh Kz + E \cosh Kz) + H + Rz^2 + Sz \tag{A-11}$$

Therefore in order to satisfy the above equation B, H, R and S must be zero. Substituting $u = 0$ at $y = a$ leads to

$$0 = A \sin Ka(D \sinh Kz + E \cosh Kz) + Fa^2 + Ga \tag{A-12}$$

This equation is satisfied if $K = m\pi/a$, and if $G = -Fa$. Therefore the velocity is now given as

$$u = Fy(y - a) + \sum_{m=1}^{\infty} \sin \frac{m\pi y}{a} \left(A_m' \cosh \frac{m\pi z}{a} + B_m' \sinh \frac{m\pi z}{a} \right) \quad \text{(A-13)}$$

The coefficient F may be determined by substituting Equation A-13 into A-1 which leads to

$$F = \frac{C}{2} = \frac{1}{2\rho\mu} \frac{dp}{dx} \quad \text{(A-14)}$$

If the boundary condition $u = 0$ at $z = 0$ is to be satisfied,

$$0 = \frac{1}{2\rho\mu} \frac{dp}{dx} y(y - a) + \sum_{m=1}^{\infty} A_m' \sin \frac{m\pi y}{a} \quad \text{(A-15)}$$

from which the coefficients A_m can be evaluated by means of Fourier's integral (69)

$$A_m' = - \frac{1}{\rho\mu a} \frac{dp}{dx} \int_0^a y(y - a) \sin \frac{m\pi y}{a} \, dy$$

$$= - \frac{2a^2}{\rho\mu m^3 \pi^3} \frac{dp}{dx} (\cos m\pi - 1) \quad \text{(A-16)}$$

The boundary condition $u = 0$ at $z = b = na$ requires that

$$0 = \frac{1}{2\rho\mu} \frac{dp}{dx} y(y-a) + \sum_{m=1}^{\infty} \sin \frac{m\pi y}{a} \left(A_m' \cosh mn\pi + B_m' \sinh mn\pi \right) \quad \text{(A-17)}$$

which when compared with Equation A-15 shows that

$$A_m' \cosh mn\pi + B_m' \sinh mn\pi = A_m' \quad \text{(A-18)}$$

whence

$$B_m' = - \frac{A_m' (\cosh mn\pi - 1)}{\sinh mn\pi} \quad \text{(A-19)}$$

Thus the final form for the velocity, u', is

$$u = \frac{1}{2\rho\mu}\frac{dp}{dx}(y - a)y + \sum_{m=1}^{\infty} \sin\frac{m\pi y}{a}(\cos m\pi - 1)\frac{2a^2}{\rho\mu m^3\pi^3}\frac{dp}{dx}$$

$$\left[\sinh\frac{m\pi z}{a}\left(\frac{\cosh mn\pi - 1}{\sinh mn\pi}\right) - \cosh\frac{m\pi z}{a}\right] \qquad \text{(A-20)}$$

This equation is the same as Equation III-31.

APPENDIX B

VERIFICATION OF THE VELOCITY PROFILE FOR A TRIANGULAR DUCT

VERIFICATION OF THE VELOCITY PROFILE FOR A TRIANGULAR DUCT

It will be shown in this Appendix that the velocity profile for a triangular duct (Equation III-38) is a solution of the governing equation (Equation III-30).

The governing equation is

$$\frac{\partial^2 u}{\partial y^2} + \frac{\partial^2 u}{\partial z^2} = \frac{1}{\rho\mu}\frac{dp}{dx} \qquad \text{(B-1)}$$

The solution of Equation B-1 for a triangular duct is (70)

$$u = -P(z + .29b)(z + 1.73\,y - .578b)(z - 1.73\,y - .578b) \qquad \text{(B-2)}$$

where P is a constant equal to $.29[dp/dx]/(\rho\mu b)$. It should be noted that this solution has not been obtained by rigorous mathematical manipulation. It should also be noted that each of the factors in parentheses in Equation B-2 is the equation of the sides of the triangle. Equation B-2 may be manipulied out to give

$$u = -P(z^3 - .867bz^2 - 3y^2z - .867by^2 + .096b^3) \qquad \text{(B-3)}$$

Thus

$$\frac{\partial^2 u}{\partial y^2} = -P(-6z - 1.732b) \qquad \text{(B-4)}$$

and

$$\frac{\partial^2 u}{\partial z^2} = -P(6z - 1.732b) \qquad \text{(B-5)}$$

Substituting Equations B-4 and B-5 into B-1 yields

$$3.46bP = \frac{1}{\rho\mu}\frac{dp}{dx} \qquad \text{(B-6)}$$

but $P = .29[dp/dx]/(\rho\mu b)$ therefore;

$$3.46b\left(\frac{.29}{\rho\mu b}\frac{dp}{dx}\right) = \frac{1}{\rho\mu}\frac{dp}{dx} \qquad \text{(B-7)}$$

which leads to the identity 1 = 1; thus Equation B-2 is a solution of Equation B-1.

APPENDIX C

A NEW SOLUTION FOR THE SKIN-FRICTION DRAG ON A CYLINDER

A NEW SOLUTION FOR THE SKIN-FRICTION DRAG ON A CYLINDER

The details of the integration of the expression for the skin-friction drag on a right circular cylinder, Equation IV-27, are given in this Appendix, and also in reference 71.

The generally accepted formulation for the skin-friction drag on a right circular cylinder is due to Thom (59,60). He calculated the skin-friction up to 60° from the forward stagnation point by using a closed form approximate solution of the boundary layer equations, and by taking values between 60° and 90° from experiment, thus deducing $3.84(\mathrm{Re})^{-\frac{1}{2}}$ as the skin-friction drag coefficient for the front half of the cylinder. With a small addition for the contribution of the rear half, Thom gave $4.0(\mathrm{Re})^{-\frac{1}{2}}$ as a close estimate of this coefficient. The analysis given in this Appendix is formulated on the basis of Blasius' solution for flow past a right circular cylinder. The integration is carried out from the stagnation point to the point of separation. The results of the integration can be arranged as a sum of easily computed terms, which heretofore has gone unnoticed.

The Blasius' velocity distribution (53) for the flow around a right circular cylinder of radius R is

$$u = 2U_\infty\left\{\left(\frac{x}{R}\right) f_1'(\eta) - \frac{4}{3!}\left(\frac{x}{R}\right)^3 f_3'(\eta) + \frac{6}{5!}\left(\frac{x}{R}\right)^5 f_5'(\eta) - \ldots\right\} \quad (C\text{-}1)$$

where x denotes the distance from the stagnation point measured along the contour of the cylinder, U_∞ is the free stream velocity and

$$\eta = y(Re)^{\frac{1}{2}}/(R) \qquad (C-2)$$

where the Reynolds number, Re, is equal to $2U_\infty R/\nu$, and y is measured perpendicular to the cylinder surface. The function $f'(\eta)$ is tabulated elsewhere (58).

The viscous drag per unit length on the cylinder may be calculated by evaluating the following integral which is the defining equation for the skin-friction drag:

$$D_F = 2\int_0^\beta \mu \left(\frac{\partial u}{\partial y}\right)_{y=0} \cos\Phi \, dx \qquad (C-3)$$

where μ is the dynamic viscosity, β is the point of separation and Φ is the angle between the tangent to the surface and the free stream velocity, Figure C-1. The position of the point of separation, β, can be found from the condition that the shearing stress must vanish at that point. For a right circular cylinder is cross flow, the point of separation has been found experimentally to be around 109° from the stagnation point. Use of the Blasius' series terminated at x^{11} leads to a separation angle of 108.8° as shown in reference 53.

Substitution of Equations C-1 and C-2 into C-3 gives

$$D_F = \frac{4\mu U_\infty}{R}(Re)^{\frac{1}{2}}\int_0^\beta \left\{\left(\frac{x}{R}\right) f_1'' - \frac{4}{3!}\left(\frac{x}{R}\right)^3 f_3''' + \ldots\right\} \cos\Phi \, dx \qquad (C-4)$$

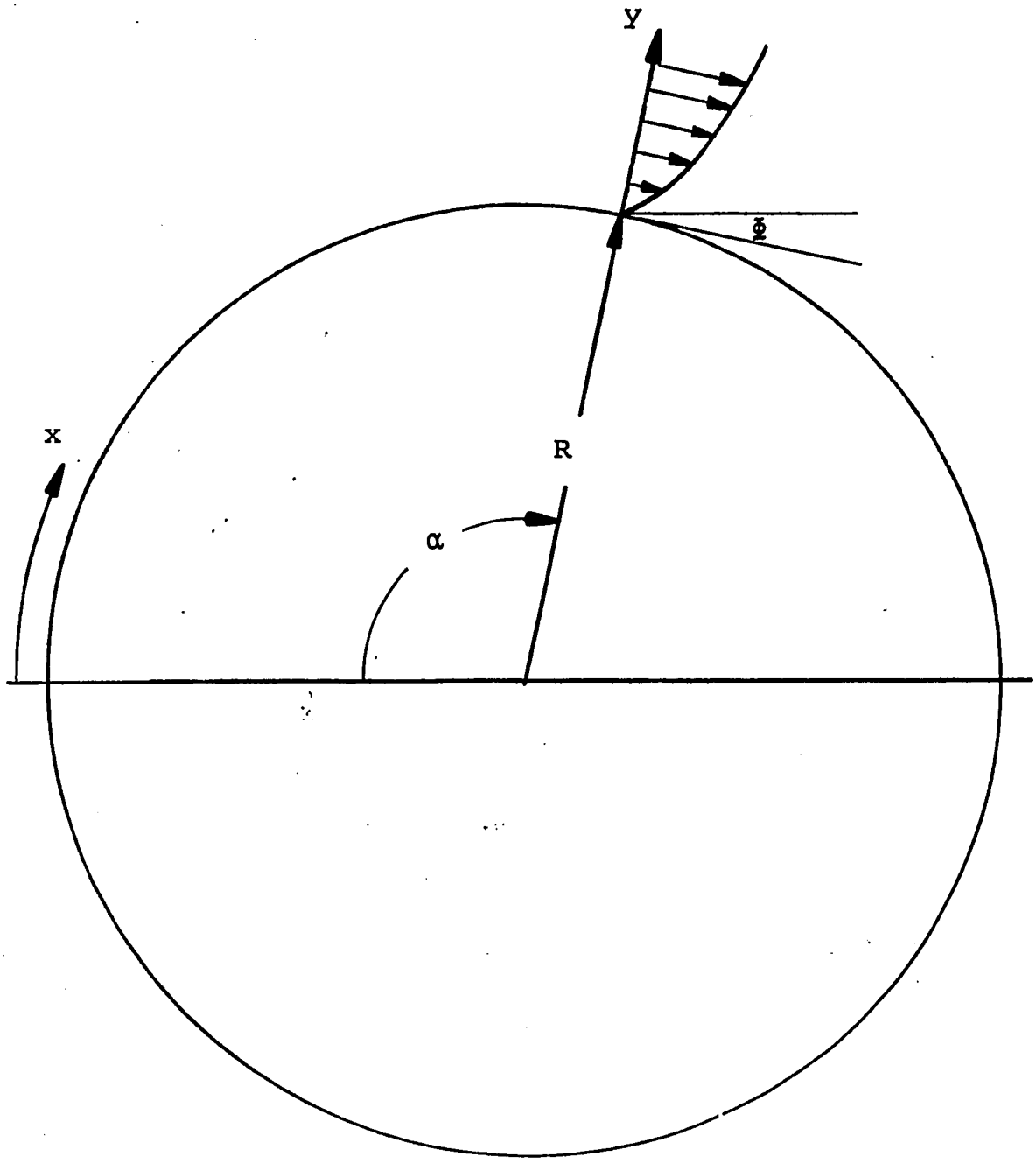

FIGURE C-1 CYLINDER CROSS SECTION SHOWING COORDINATE REFERENCES AND ANGLES

This integral may be evaluated by noting that $\cos\Phi = \sin\alpha$ (Figure C-1) and $\alpha = x/R$; therefore,

$$D_F = 4\mu U_\infty (Re)^{\frac{1}{2}} \int_0^\beta \left\{ f_1'' \alpha - \frac{4}{3!} \alpha^3 f_3'' + \ldots \right\} \sin\alpha \, d\alpha \qquad (C\text{-}5)$$

or

$$D_F = 4\mu U_\infty (Re)^{\frac{1}{2}} \left[f_1'' \int_0^\beta \alpha \sin\alpha \, d\alpha - \frac{4}{3!} f_3'' \int_0^\beta \alpha^3 \sin\alpha \, d\alpha + \ldots \right] \qquad (C\text{-}6)$$

The integrals in Equation C-6 may be evaluated by successive integration by parts, which leads to

$$\begin{aligned} D_F = 4\mu U_\infty (Re)^{\frac{1}{2}} \Big[& f_1'' (- \beta \cos\beta + \sin\beta) \\ & - \frac{4}{3!} f_3''(- \beta^3 \cos\beta + 3\beta^2 \sin\beta + 6\beta \cos\beta - 6 \sin\beta) \\ & + \frac{6}{5!} f_5''(- \beta^5 \cos\beta + 5\beta^4 \sin\beta + 20\beta^3 \cos\beta - 60\beta^2 \sin\beta \\ & - 120\beta \cos\beta + 120 \sin\beta) + \ldots \Big] \end{aligned} \qquad (C\text{-}7)$$

Equation C-7 may be rearranged to give

$$\begin{aligned} D_F = 4\mu U_\infty (Re)^{\frac{1}{2}} \Big[& f_1'' (\sin\beta - \beta \cos\beta) \\ & + 2 \left(\frac{\sin\beta}{0!} - \frac{\beta \cos\beta}{1!} \right) \left(2f_3'' + 3f_5'' + 4f_7'' + 5f_9'' + 6f_{11}'' + \ldots \right) \\ & - 2\beta^2 \left(\frac{\sin\beta}{2!} - \frac{\beta \cos\beta}{3!} \right) \left(2f_3'' + 3f_5'' + 4f_7'' + 5f_9'' + 6f_{11}'' + \ldots \right) \\ & + 2\beta^4 \left(\frac{\sin\beta}{4!} - \frac{\beta \cos\beta}{5!} \right) \left(3f_5'' + 4f_7'' + 5f_9'' + 6f_{11}'' + \ldots \right) - \ldots \Big] \end{aligned} \qquad (C\text{-}8)$$

Equation C-7 may also be written using summation notation as

$$D_F = 4\mu U_\infty (Re)^{\frac{1}{2}} \left[f_1'' (\sin\beta - \beta\cos\beta) \right. \tag{C-9}$$
$$\left. + 2\sum_{m=1}^{m=\infty} \left\{ (m+1)\, f''_{2m+1} \left(\sum_{n=0}^{n=m} (-1)^n \beta^{2n} \left[\frac{\sin\beta}{(2n)!} - \frac{\beta\cos\beta}{(2n+1)!} \right] \right) \right\} \right]$$

The viscous drag coefficient is defined as

$$C_{D_F} = \frac{D_F}{\frac{1}{2}\rho U_\infty^2 D} \tag{C-10}$$

where ρ is the density. Hence substituting Equation C-9 into C-10 gives

$$C_{D_F} = \frac{8}{(Re)^{\frac{1}{2}}} \left[f_1'' (\sin\beta - \beta\cos\beta) \right. \tag{C-11}$$
$$\left. + 2\sum_{m=1}^{m=\infty} \left\{ (m+1)\, f''_{2m+1} \left(\sum_{n=0}^{n=m} (-1)^n \beta^{2n} \left[\frac{\sin\beta}{(2n)!} - \frac{\beta\cos\beta}{(2n+1)!} \right] \right) \right\} \right]$$

The above coefficient is tabulated in Table C-I for various degrees of approximation. As can be seen from the table, the coefficient appears to be converging to 6 $(Re)^{-\frac{1}{2}}$, which is depicted in Figure C-2.

This analysis gives a value of 6 $(Re)^{-\frac{1}{2}}$ for the skin-friction drag coefficient; whereas, Thom's approximate theory gives a value of 4 $(Re)^{-\frac{1}{2}}$. Both values are plotted in Figure C-2 along with the experimental data of Linke (72). Caution should be taken in drawing conclusions from the data of Linke as drawn in Figure C-2 since it is calculated from experimentally

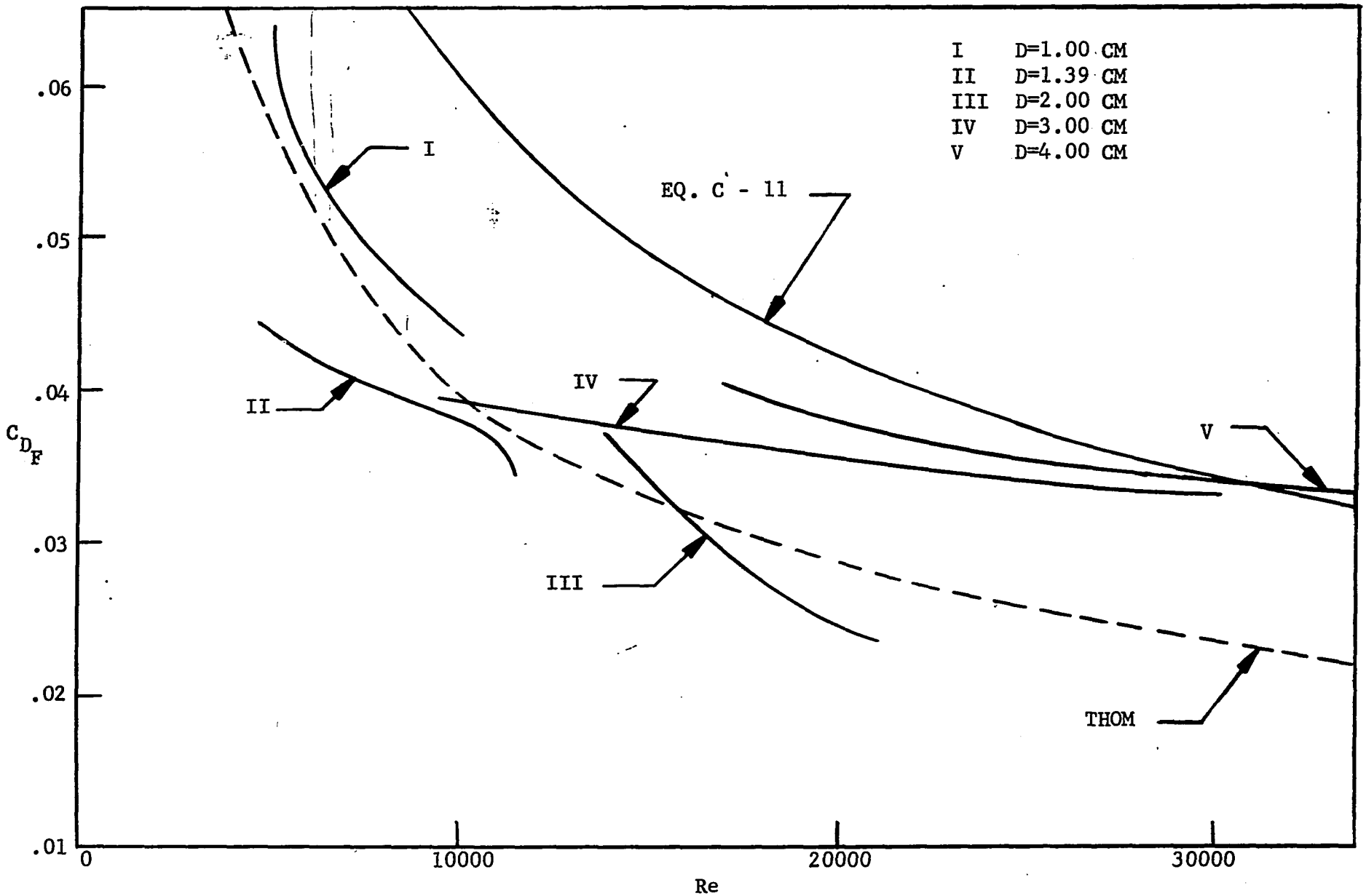

FIGURE C-2 COMPARISON OF SKIN-FRICTION DRAG COEFFICIENT WITH THEORY OF THOM AND DATA OF LINKE

obtained results for the total and pressure drag coefficients and not by direct measurements of the skin-friction. Figure C-3 is a typical plot of the data of Linke for total and pressure drag coefficients. As can be seen from this figure, calculation of the skin-friction drag is very arbitrary due to the scatter in the data.

Table C-1 Skin-Friction Drag Coefficient For Various Degrees of Approximation

$C_{D_F}(Re)^{\frac{1}{2}}$	Approximation
15.3880	through x
3.4016	through x^3
6.5448	through x^5
6.0096	through x^7
6.0136	through x^9
5.9856	through x^{11}

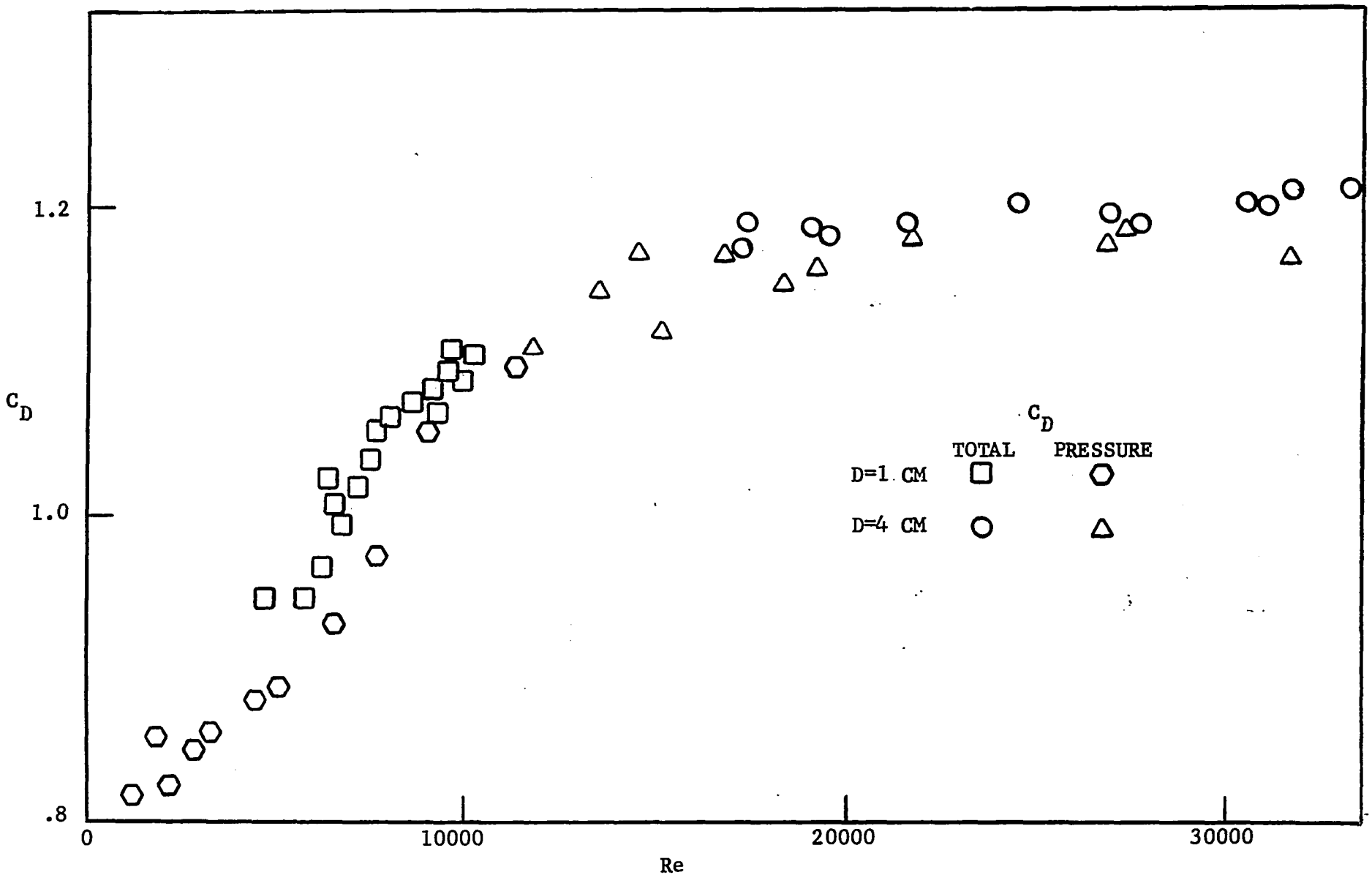

FIGURE C-3 LINKE'S DATA FOR TOTAL AND PRESSURE DRAG COEFFICIENTS

VITA

The author was born in New Orleans, Louisiana, on June 4, 1938. He attended Our Lady Star of the Sea Elementary School and was graduated from John McDonogh Senior High School, New Orleans, in June, 1956. He received the American Legion Award for the outstanding graduate.

His undergraduate work was at Tulane University in New Orleans. He received the Bachelor of Science degree in Electrical Engineering from that institution in June, 1960. In September, 1960, he entered the Tulane Graduate School and proceeded with work on the Master of Science degree in Mechanical Engineering, which he received in August, 1962. He is now a candidate for the degree of Doctor of Philosophy at Louisiana State University in Baton Rouge.

He is a member of the American Society of Mechanical Engineers, the American Institute of Aeronautics and Astronautics, the American Society for Engineering Education, the physics honor society - Sigma Pi Sigma, and the research society - Sigma Xi.

He is married and has three children.

EXAMINATION AND THESIS REPORT

Candidate: Edwin Price Russo

Major Field: Mechanical Engineering

Title of Thesis: "On a New Approach to Rarefied Flow With Applications to Certain Classical Problems"

Approved:

Major Professor and Chairman

Dean of the Graduate School

EXAMINING COMMITTEE:

Date of Examination:

December 11, 1967